Fluidized bed agglomeration inhibition by additives during combustion of demanding biomass fuels

Thesis for M.Sc. in Chemical Engineering

by

Alex Söderholm

Laboratory for Inorganic Chemistry

Faculty of Science and Engineering

Åbo Akademi University

September 2022

Abstract

Title of the thesis:	Fluidized bed agglomeration inhibition by additives during combustion of demanding biomass fuels
Author:	Alex Söderholm
Thesis supervisors:	Dr Patrik Yrjas *Åbo Akademi University, Turku Finland* Dr Emil Vainio *Åbo Akademi University, Turku Finland*
Date and place:	September 30, 2022

Bed agglomeration is a problem related to fluidized bed combustion. It is a result of bed particles and/or fuel ash gluing together, forming agglomerates, i.e., large clusters. These agglomerates can, over time, increase in the bed to the point where the fluidization of the bed is affected. In the case of defluidization or collapse of the bed, a boiler would have to be shut down for maintenance. It is mainly a problem related to burning biomass, especially those exhibiting large amounts of alkali. Researchers have made significant efforts to find preventive measures to avoid a costly shutdown of boilers.

There are two main mechanisms causing agglomeration. Coating-induced agglomeration is a result of reactions between the fuel ash and the bed material. This results in a coating on the bed material. In comparison, melt-induced agglomeration stems directly from the ash-forming matter, and a melt is formed from compounds within the fuel ash. In both cases, the melt then acts as a glue between bed particles resulting in interparticle forces. When this interparticle force exceeds the forces pulling them apart, agglomerates can form. Additives, such as kaolinite, have been shown to prevent melt-formation. This is attributed to the capture of alkali in the case of kaolinite, thus preventing it from forming molten alkali-silicates.

The main research objectives for this thesis were the following:

- Determining the inhibiting effects of limestone and kaolinite
- Expand upon the knowledge of agglomerations mechanism and the influence of additives
- Determine the amount of additive to prevent agglomeration

Initially, a literature review was conducted to review the current state of research in the area. This included understanding the bed agglomeration phenomena itself as well as current methods for preventing it. In addition, an experimental campaign was conducted with a laboratory-scale fluidized bed reactor. The campaign aimed to determine the influence of temperature and additives on agglomeration. Sunflower seed shells and wheat straw were used as fuels, while kaolinite and limestone were used as additives. Samples from the spent bed were analyzed with scanning electron microscopy and x-ray spectroscopy.

The results show that kaolinite is a proficient countermeasure for agglomeration. The effect is dependent on the agglomeration mechanism. It works better in the case of coating-induced agglomeration. With melt-induced agglomeration, the initiation was delayed but not completely avoided.

Limestone did not yield any significant improvement compared to tests without additives.

Keywords: bed agglomeration, fluidized bed combustion, biomass, additive, defluidization

Acknowledgments

This work has been carried out within the CLUE^2-project (2017-2022). Support from ANDRITZ Oy, Valmet Technologies Oy, UPM-Kymmene Oyj, Metsä Fibre Oy, and International Paper Inc. is gratefully acknowledged.

I would like to express my sincere gratitude to both of my excellent supervisors Patrik Yrjas and Emil Vainio. I am extremely grateful for all the help and support, it would not be possible without your input. I would also like to extend my gratitude to other OOK members who helped me along the way in different ways, especially Tor Lauren and Mehretu Dirbeda. Also a big thanks to Linus Silvander for conducting all the SEM- and XRD-analyses for me.

Finally, I would like to thank my wife Pinja for always being supportive. All in all, it took a long time to get here, one of my favorite sayings in Swedish is probably appropriate to describe the process: “Väntar på något gott blir det skönt sen!”.

Abbreviations

BECCS bioenergy with carbon capture and storage

BFB bubbling fluidized bed

CFB circulating fluidized bed

EDS energy-dispersive X-ray spectroscopy

FBC fluidized bed combustion

SEM scanning electron microscope

SFSS sunflower seed shell husk

Table of Contents

List of Figures

List of Tables

1 Introduction

Global warming has since long been a well-known fact. The consequences are alarming and could lead to a rise in sea level, a significant increase in extreme weather phenomena, and an adverse effect on biodiversity. Biomass waste streams and fast growing biomasses offer a carbon-neutral option for the replacement of anthropogenic emissions in the energy sector, as long as it is done in a sustainable manner (Clarke et al., 2022).

Biomass has been a long-debated subject in light of the proposed carbon neutrality. The argument at hand is that the natural circulation of carbon is simply expedited. Biomass captures CO_2 using photosynthesis as part of the growth cycle. In the natural process, this carbon would be stored in the plant until the inevitable decay at the end of life. Carbon would be slowly released during the breakdown of the plant matter. Upon use as a fuel in a combustion process, this process is highly expedited, resulting in a fast release of the same carbon while also capturing the stored energy. One must put this in the proper perspective and make the comparison to the use of fossil fuels that unequivocally result in more carbon dioxide in the atmosphere. There are possible adverse effects in the utilization of biomass which can be mitigated by sustainable growing practices. In combination with carbon capture, Bioenergy with carbon capture and storage, BECCS, will result in a negative net effect on emissions (Clarke et al., 2022).

Fluidized bed combustion is the leading technique used in the combustion of biomass, offering several benefits over grate-fired boilers. These are mainly high fuel flexibility, i.e., good tolerance for moisture in fuel, as well as higher efficiency. However, the main drawback, as compared to other techniques, is the agglomeration of the fluidized bed which can result in unscheduled shutdowns. Agglomeration refers to bed particles gluing together, forming bigger particles. When reaching a critical amount and mass, these will disturb the fluidization of the bed (Basu, 2006).

As the demand for biomass in different applications is rising steeply, previously underutilized or unused sources are suddenly part of the consideration. These byproducts, residues, and waste-based fuels have a distinct set of problems from the relatively higher fraction of ash-forming matter in addition to being more troublesome regarding composition.

In a study at Åbo Akademi, the inhibiting effect of peat on bed agglomeration during the firing of demanding biomass was reported (internal report CLUE^2-project). The fuels used in that study have different agglomeration mechanisms. The ash-forming elements either reacted directly with the sand bed forming a low melting silicate, while the ash-forming elements of wheat straw in the fuel reacted with each other, forming a low-melting silicate which then caused agglomeration (Sevonius, 2021).

The previously used fuels were sunflower seed shells (reaction with bed material) and wheat straw (reaction between ash elements). When fired together with peat, it seems that the Ca and the Al-silicates in peat inhibit the agglomeration rate, while sulfur was found not to play a significant role. Furthermore, the previous results indicated that the inhibiting effects were more pronounced in the mechanism where the ash-bed reaction was dominant, compared to the ash-ash agglomeration mechanism (Sevonius, 2021).

This thesis aims to confirm the inhibiting effects of Ca and Al-silicate by mixing limestone ($CaCO_3$) and kaolinite (Al-silicate) into the bed. The purpose is to use the same fuels as previously and compare the effects and verify the previous results with peat and determine the amounts of additives needed to inhibit agglomeration.

The main research objectives for this thesis were the following:

- Determine the inhibiting effects of Ca and Al-silicates
- Expand upon the knowledge of agglomerations mechanism and the influence of additives
- Determine the amount of additive to prevent agglomeration

The structure of the thesis is as follows. Chapter 2 covers biomass as a fuel covering its general composition, with special attention given to the ash-forming matter and its behavior. In addition, fluidized bed combustion technologies are covered. Chapter 3 is a review of the current state of knowledge regarding bed agglomeration and its prevention. Chapter 4 covers the experimental part of this thesis: lab-scale experimental reactor, fuels, and additives used in the test run as well as consequential analysis of obtained samples. The results of the experiments are discussed and analyzed in chapter 4. Finally, the whole thesis is summarized and concluded with suggestions for further research in chapter 5

2 Combustion of biomass in fluidized beds

This chapter will provide the theoretical background for the thesis, provide background on the specifics of fluidized beds, and discuss biomass as a fuel. Fluidized bed combustion will be discussed from a technological viewpoint, outlining its benefits and drawbacks. The focus regarding biomass will be on the ash-forming matter, its behavior and composition, as it is of paramount importance when discussing agglomeration.

2.1 Principles of fluidized beds

Fluidized bed combustion boilers (FBC) were commercialized in the 1970s and have since seen significant improvements and widespread adoption as one of the leading technologies in the combustion of solid biomass fuels. A fluidized bed revolves around the idea of a bed of particles with gas flowing through it, thus, exhibiting a liquid-like behavior (Leckner, 2016).

In principle, the particles in the bed are subjected to two forces, the gravitational pull, and the upward force of the gas. The bed behaves differently depending on the gas velocity, and it can be divided into four different regimes. In literature, different names can be used for several of the regimes, as well as models describing more than four distinct phases. For this thesis, a model presented by Basu (2006) was chosen. The bed can be regarded as fluidized when the gas flow creates a drag force that exceeds the gravitational force and suspends the particle. At lower gas velocities, the bed is regarded as a packed bed. At the minimum fluidizing velocity, U_{mf}, the particles are suspended, and the volume of the bed increases. The bed can be regarded as a bubbling bed. Further increasing the velocity leads to a turbulent bed where the velocity is close to the terminal velocity of the particles. Big voids are formed in the bed, and the bed does not exhibit a distinct surface. As the gas velocity increases to the terminal velocity, the particles in the bed are no longer retained in the bed but instead transported in the gas phase. At this stage, the bed becomes a fast or turbulent fluidized bed. In a boiler, these particles must be recovered from the gas and returned to the bed. The different regimes are a simplification of reality, and in practice, the boundaries are not very clearly defined. However, it acts as a general framework when discussing fluidization (Basu, 2006; Raiko, 2002).

The minimum fluidization velocity, U_{mf}, is influenced by several parameters, such as particle diameter, particle shape, and gas density. Geldart (1972) presented a classification system for the fluidization of particles, incorporating particle size and the difference in particle density and gas density which are essential for the fluidization behavior. The classification system can be seen in Figure 1. The x-axis has the particle's diameter, and the y-axis is the difference between the particle and fluidizing medium.

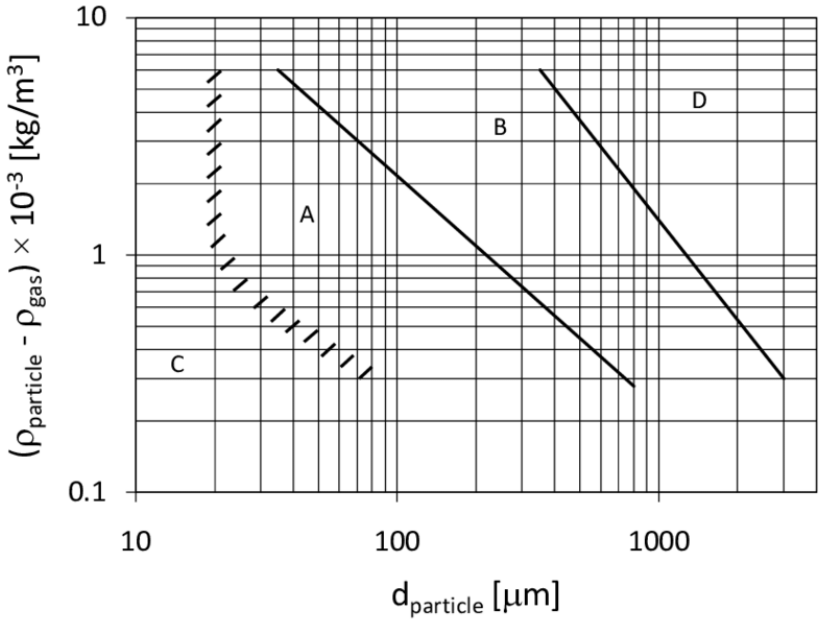

Figure 1 Powder classification (Drake, 2011) adopted from Geldart (1972).

Group C particles consists of very fine particles, smaller than 30 µm (ρ_p = 2500 kg/m^3). These particles are generally difficult to fluidize due to interparticle forces comparable to the gravitational force. Group A particles typically consists of particles in the range of 30–100 µm (ρ_p = 2500 kg/m^3) which are easy to fluidize. Group B particles typically consists of particles in the range of 100–500 µm (ρ_p = 2500 kg/m^3), which fluidize well. This is the most common particle size for fluidized bed boilers. The bubbling velocity is close to that of U_{mf}. Group C consists of particles >500 µm (ρ_p = 2500 kg/m^3) and requires a significantly higher velocity to fluidize (Basu, 2006).

2.2 Fluidized bed combustion technologies

There are two main types of fluidized boiler technologies in use, Bubbling Fluidized Bed, BFB, and Circulating Fluidized Bed, CFB. BFBs are better suited for fuels with a high share of volatiles, such as biomass. CFBS, on the other hand, are more suited for operation with fuels that have a high amount of fixed carbon, such as coal. Figure 2 shows a schematic illustration of the two technologies (Leckner, 2016).

Fluidized bed boilers have several advantages over other types of solid fuel-fired boilers. At a time, only 1–3% of the bed consists of fuel particles, while the rest is noncombustible solids made up of the bed material and ash particles. This gives high flexibility regarding different fuel qualities. The conditions lead to a very good solid-solid and gas-solid mixing, providing fast dispersion and ignition of the fuel without impeding the temperature. Due to the good mixing of the gas-solid phase, high efficiency of the combustion process is achieved, 90–98% for BFB and even higher for CFB, 97.5-98%. Relatively low furnace temperatures use of extensive air-staging allow for reduced NO_x emissions. SO_2 can also be removed directly from the furnace with limestone (Basu, 2006).

BFB boilers are operated at lower gas velocities, 1–2 m/s, in the bubbling regime and utilize group B Geldart particles. It can be divided into three principal sections: bed, freeboard, and the convection or backpass section (Leckner, 2016).

CFB boilers operate in the fast fluidization regime and utilize group A Geldart particles. In practical terms, the fluidization regime is dependent on the height. Closer to the bed itself, the operation is close to bubbling, but when the height increases, the regime shifts to a fast fluidized bed. The fluidization velocity is 5–6 m/s, and a cyclone is used to capture the bed particles from the gas phase. These particles are then returned to the bed through a loop seal (Leckner, 2016).

BFB and CFB boilers have somewhat different use cases, the former usually in the range of 10–100 MW_{th} and later in 50–600 MW_{th}. BFB boilers offer lower investment costs due to the more straightforward construction and design, and they are, in general, used for highly volatile biomass. A CFB boiler achieves less NO_x and SO_x and has a higher combustion

efficiency and higher flexibility in the choice of fuels. In addition, the load can be adjusted quicker, which allows for a more flexible operation (Basu, 2006; Leckner, 2016).

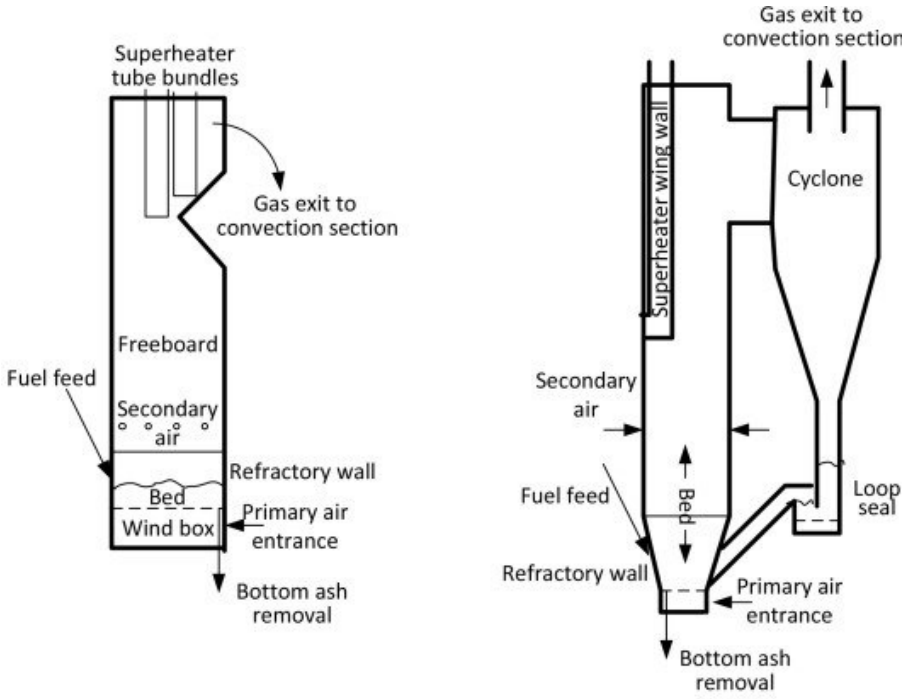

Figure 2 A schematic illustration of the BFB (left) and CFB (right) (Modified from Leckner, 2016).

2.3 Biomass as a fuel

Biomass is defined as biological matter from living or dead organisms. In principle, everything originating from photosynthesis is considered biomass. It comprises both inorganic and organic material as it originated from both vegetation and living organisms (Vassilev et al., 2010). The categorization of biomass presents some challenges due to the considerable variation in properties, and a wide variety of sources and quantities. There is hence no unilateral way of categorization. The situation is mainly dictating a suitable division. In general, biomass is either divided based on the origin or based on the specific use (Tursi, 2019). Vassilev et al. (2010) presented the following division based on the origin:

1. Wood and woody biomass
2. Herbaceous and agricultural biomass
3. Aquatic biomass
4. Animal and human biomass wastes

2.3.1 Ash-forming matter

Ash can be defined as the incombustible rest of the fuel that remains after complete combustion. However, the ash-forming matter will react through different paths forming complex compounds. The essential ash-forming elements in biomass are Si, Ca, Mg, K, Na, P, S, Cl, and Al, regarding ash-related reactions and consequential problems. The quality and quantity of the ash depend heavily on the fuel and is combustion technology, and eventual additives (Boström et al., 2012).

Traditionally, fuels have been analyzed by proximate (moisture, ash, volatile matter, and fixed carbon) and ultimate analysis (carbon, hydrogen, oxygen, nitrogen, and sulfur). As a simplification, the ash components are usually reported in their oxide form. The reactivity of the different species found in the ash-forming matter is, however, highly dependent on the forms in which they are bound in the fuel. Chemical fractionation can be used to differentiate this. The three-step process involves the leaching of water, ammonium acetate, and hydrochloric acid, consequently. The leaching results in three fractions and one solid fraction being the insoluble residue left over (Zevenhoven et al., 2012).

The ash-forming elements can, in general, be divided into four different groups: minerals, both included and excluded, organically associated matter, and dissolved salts. Included minerals are in the structure because of natural processes occurring during the growth. Minerals such as silica, calcium oxalate, and phosphates are precipitated into the structure. Excluded minerals are a result of impurities that are not part of the biomass itself. These contaminants are incorporated into the fuel during processing, harvesting, and growth and are generally made up of sand and clay minerals, and are, in general, less reactive than included minerals. Dissolved salts are found dissolved in liquids in the biomass. These consist of different ions. Upon drying, they will precipitate but will remain soluble. The organically associated matter is bound to the carbon-rich structure, i.e., mainly metal ions bound to anionic groups. (Boström et al., 2012; Zevenhoven et al., 2012).

The ash-forming matter and, in extension, the ash is the main contributor to operational issues in boilers. It contributes to slagging, fouling, corrosion, and agglomeration and might eventually result in an unscheduled downtime of the boiler. The behavior of a particular fuel

is difficult to predict even if prediction models could offer an indication. In the following section, the reactions related to the main components in ash will be described.

2.3.2 Reactions of the ash-forming matter

Several influencing variables play an essential role when considering the ash-forming elements and their reactions. Reaction equilibrium and the phase of the ash are also highly dependent on the specific stage of the combustion since the conditions vary a lot, i.e., temperature and gas composition. Boström et al. (2012) divide these reactions into two stages: primary ash transforming reactions which are seen to involve oxygen and relate to the initial reactions. The secondary ash transformation is a reaction where compounds formed in the initial stages of combustion react trough out the boiler.

Silicon in the biomass ends up as an insoluble residue in the ash and is found as silica (SiO_2) and different silicate minerals in the ash. These are, in general, not problematic under FBC conditions due to the high melting point. Alkaline earth metals present in the ash-forming matter could, however, influence them. A combination of the different elements could lead to silicates with a melting temperature that would cause problems under FBC conditions. Alkali vapors are formed among the immediate reactions in the initial stages. These then take part in the formation of alkali silicates with a low melting point. The formed alkali silicates can be either solid or liquid, depending on the temperature. Reaction equation 1 below shows an example of a reaction with silica and alkali vapor (Boström et al., 2012; Zevenhoven et al., 2012).

$$\mathrm{SiO_2(s)} + 2\,\mathrm{KOH(g)} \leftrightarrow \mathrm{K_2SiO_3(s,l)} + \mathrm{H_2O(g)} \quad (1)$$

Si and K can be found in equal amounts in agricultural wastes such as hulls and different straws and could thus contribute to the behavior described above. Silica and K found in the insoluble rest after chemical fraction should not be considered less reactive.

Zevenhoven et al. (2012) state that potassium is the single most crucial element in the ash-forming matter when considering problems in the fireside in biomass boilers. Potassium can be found in both reactive and unreactive forms in fuels. The reactivity can be estimated with chemical fractionation. Potassium is mainly present as an organically associated ion bound to active groups or as salt in fluids. Sodium is often grouped with potassium as their reaction

paths are very similar. The K found in biomass-based fuels is, in general, soluble in water and is primarily released as gaseous KCl (g), KOH (g), and K(g). The formations of the different gases are dependent on the partial pressure of oxygen and the presence of chlorine. Oxidative conditions favor the formation of KOH (g). If chlorine is present, the primary vapor formed is KC l(g). The formation of vapor is considered a primary reaction and is followed by a secondary reaction involving the vapors that are formed. Sulfur has a significant effect on the reactions of the alkali vapors. SO_3(g) reacts with KCl (g) and KOH (g), which further reacts to KSO_3Cl and $KHSO_4$, resulting in the reactions described in Equations 3 and 4 (Glarborg and Marshall, 2005).

$$\mathrm{KS}O_3\mathrm{Cl(g)} + H_2\mathrm{O(g)} \leftrightarrow \mathrm{KHS}O_4\mathrm{(g)} + \mathrm{HCl(g)} \quad (2)$$

$$\mathrm{KHS}O_4\mathrm{(g)} + \mathrm{KCl(g)} \leftrightarrow K_2SO_4\mathrm{(g)} + \mathrm{HCl(g)} \quad (3)$$

Aluminum naturally occurring in biomass is usually organically bound and is mainly inert when considering ash chemistry. Different impurities might, however, introduce alumina in the form of silicates, e.g., clay (Zevenhoven et al., 2012). The aluminosilicates can react with the alkali metals and form high melting aluminosilicates, which would have a beneficial effect on slagging (Boström et al., 2012).

Calcium is the most abundant element in the ash-forming matter of woody biomass (Vassilev et al., 2017). Organically bound Ca can, when heated, form CaO. The particles are considered small and will be in the micrometer range. CaO participates in further reactions, with the main one to be considered sulfation, described by equation 5 (Zevenhoven et al., 2012).

$$\mathrm{CaO(s)} + \mathrm{SO_2(g)} + \frac{1}{2}\,\mathrm{O_2(g)} \leftrightarrow \mathrm{CaSO_4(s)} \quad (4)$$

Calcium is sometimes added in the form of limestone for this specific reaction to mitigate SO2 from the flue gases. Limestone reacts similarly to the organically bound Ca in the fuel. The capture of SO2 also affects the other reactions present, mainly the sulfation of alkali chlorides described above in reactions 3 and 4. Recarbonation of CaO also plays a role. The reaction can be seen in equation 6. It might lead to fouling problems through sintering in the flue gas system, e.g., in the cyclone. This reaction is seen at temperatures between 600 to 800 °C (Leckner, 2016).

$$CaO(s) + CO_2(g) \leftrightarrow CaCO_3(s) \quad (5)$$

Magnesium is less abundant than Ca in biomass and reacts similarly to Ca. However, it is less reactive and does not play a significant role in the fireside of the boiler (Zevenhoven et al., 2012).

Phosphorus is found in biomass as organic molecules, which contain P, e.g., phytic acid, or as phosphate salts, e.g., K_3PO_4. The amount varies significantly between different types of biomasses, but it is, in general, high in annual biomasses (Vassilev et al., 2017). Phosphorus reacts with both alkali metals and Ca. Phosphorus forms high melting compounds when it reacts with Ca that do not cause any significant problems. However, the reactions with alkali might lead to problems since low-melting eutectic mixes are formed, which may induce agglomeration of the bed (Grimm et al., 2011).

3 Agglomeration mechanisms

A comprehensive approach is needed to study and quantify bed agglomeration. It involves chemical reactions, hydrodynamics, and interaction between the bed and the ash. This complex system thinking has resulted in a plethora of different approaches, and consequently, there are also different terms explaining similar reactions (Khadilkar et al., 2016).

There is extensive literature concerning ash-induced agglomeration (e.g., Visser et al., 2004 and Gatternig and Karl, (2015). The root cause of bed agglomeration is ash with low melting points, which then forms a glue-like coating on the bed particles resulting in interparticle forces. When this interparticle force exceeds the forces pulling them apart, agglomerates can form. The agglomerates affect the hydrodynamic conditions in the bed, increasing the $U_{mf,}$ as discussed in section 2.2. The agglomeration precedes with time until the agglomerates cause a complete defluidization (Gatternig and Karl, 2015).

Visser (2004) was the first researcher to name the two significant agglomerations mechanisms related to biomass combustion in FBC as coating-induced and melt-induced agglomeration. Figure 3 gives a schematic overview of these mechanisms, which will be described in the two following sections.

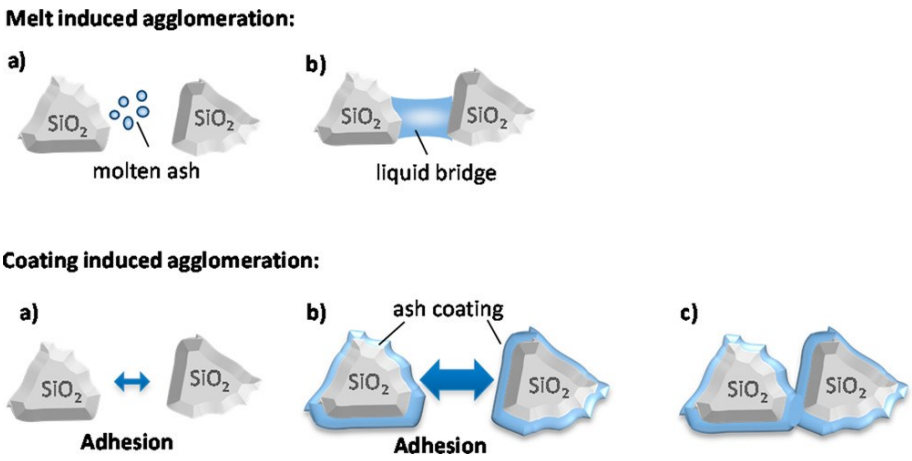

Figure 3 The agglomeration framework describing the two major agglomeration mechanisms presented by Gatternig and Karl (2015) and originally adopted from Visser (2004).

3.1 Coating-induced agglomeration

A three-step process was put forth in work by Öhman and Nordin (2000). The phenomena were studied in a laboratory-scale fluidized bed that was heated at a steady rate until defluidization was detected. They found that the primary constituents in addition to silica in the coating of the bed particles were potassium and calcium. As a result of this study, they proposed the following mechanism leading to agglomeration of the bed:

1. The ash deposits on bed material particles. Three different reaction paths are presented for the coating of the particle, including attachment of small ash particles, reactions between gaseous alkali species and the bed material, and condensation of gaseous alkali species on the surface of the bed material.
2. A uniform coating is formed on the bed particle as the molten phase on the particle's surface grows and homogenizes.
3. The molten layer consisting of silicates adheres to bed particles and forms agglomerates in a temperature-controlled process.

A similar mechanism is elaborated on and expanded in several other publications, such as Visser (2004), Brus (2005), and Nuutinen (2004). There is, however, some debate regarding the viability and exact pathways of the formation and transportation of the ash to form deposits. Gatternig and Karl (2015) studied the impact of gaseous alkali species in a reactor with a separate fluidized bed of sand above a fixed bed with the fuel. They did not observe any layer formation in the fluidized bed, thus, implying that volatile alkali species would not play a role in the formation of a coating layer. This conclusion was based on the isothermal nature of a fluidized bed. In practice, local hot spots can be formed in a bed. These local hot spots and temperature gradients could provide a pathway for evaporation-condensation to occur and put some doubt upon the mentioned findings. Figure 5 presents a schematic view of the three different pathways for depositions formation on the bed particles. This includes attachment of molten ash, impaction of small ash particles, and reactions occurring with gaseous alkali metal species. The solid particles are attached using wan der Waals forces. These particles are small, <10 μm. The molten ash particles can be attached upon collision and are liquid-induced and driven by viscous lubrication and capillary forces (Gatternig and Karl, 2015).

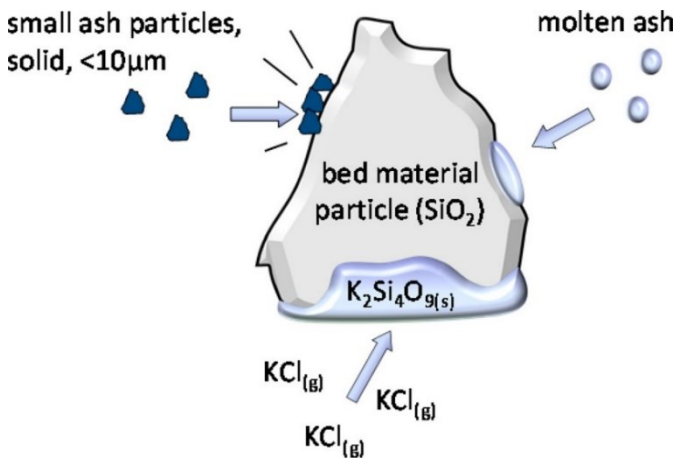

Figure 5 Transportation mechanism for the ash (Gatternig and Karl, 2015).

Regardless of the specific initial transportation mechanism of the ash to the surface, there is the growth of the layer over time. The layers also typically form a clear two- or three-layered coating with distinct differences in chemical and structural composition between layers (Gatternig and Karl, 2015). The overall thickness of the coating reported in the literature varies from 1 to 50 µm, with some reporting up to 70 µm thick deposits. (Nuutinen et al., 2004; Visser et al., 2004). An example of the compositions of a two- and three-layer coating can be seen in Figure 4, with a K-lean system on the left and a K-rich system on the right.

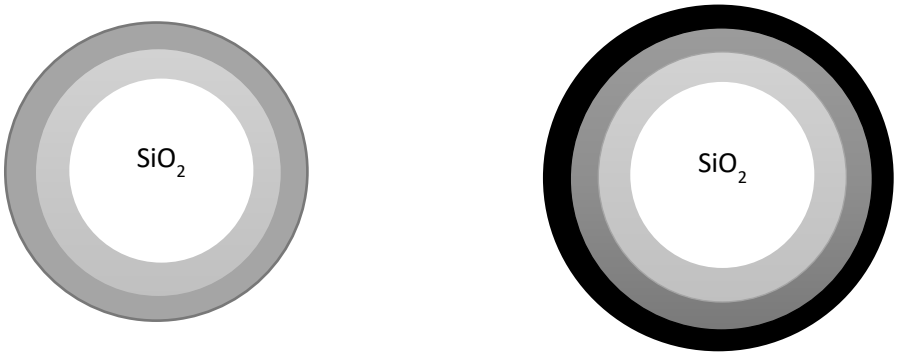

	Inner	Outer
Element	wt-%	wt-%
Si	14	3
Ca	41	28
P	-	5
K	-	7
S	-	4

	Inner-inner	Inner	Outer
Element	wt-%	wt-%	wt-%
Si	34	14–18	3
Ca	4–5	44	29
P	-	-	6
K	10	-	7
S	-	-	4

Figure 4 Representation of the layering formation adopted from Visser (2004).

Over time distinct layering can be observed on the coating of the bed particles. The layer formation is highly dependent on the fuel composition. Differences in morphology can also be observed between the layers. In a two-layer coating, the outer layer is usually granular, and the composition is reminiscent of the global ash composition (Visser et al., 2004). Gatternig and Karl (2015) further expand upon the characterization of the layered deposits describing an inner layer that is homogenous and consists of Ca- and K-silicates. The morphology suggests that the inner layer is responsible for the agglomeration due to it being similar to the composition of the neck gluing the particles together. The outer layer is depleted of Ca and K, indicating that these elements, as more reactive components, are transported by diffusion towards the Si-core. An outer third layer has been observed and is noted to be rich in calcium and magnesium. The layer is suggested to inhibit agglomeration (Nuutinen et al., 2004).

As already alluded to, the structure, thickness, and composition of the layer are dependent on time. He et al. (2014) put forward a framework for the build-up and growth of the coating divided into three stages. The study was conducted with three different boilers, a lab-scale 5 MW_{th} BFB, a 30 MW_{th} BFB, and a 122 MW_{th} CFB with woody biomass as fuel. Bed samples were taken out at specific intervals during the operation to study the layer growth over time.

The initial stage resulted in a single layer and could be observed on samples up to a day old. The layer was relatively thin and homogeneous. Initial reactions involve potassium species forming a low melting potassium silicate. (He et al., 2014).

The second stage resulted in the formation of different layers within the coating. The molten silicates facilitate the adhesion of ash particles on the surface. The K/Ca proportion decreased over time, as Mg and Ca species adhere and dissolve into the molten phase. The layer growth also continued inwards as the alkali species reacted with the silica. As the diffusion of these species slowed down over time, the growth inward of the inner layer also slowed down. This phase took place between one and two weeks (He et al., 2014).

In the last and third stages, from two to three weeks, the layer growth slowed down substantially. A third layer that consisted mainly of Ca-silicates was formed on the surface (He et al., 2014).

Distinct differences between BFB and CFB could also be observed in the layer formation. The outer layer of the particles from CFB was thinner and was attributed to the higher erosion present in a CFB boiler. As there was less Ca present to diffuse, the K/Ca ratio was higher in the inner layer for the particles from the CFB (He et al., 2014).

In addition to the layer growth outwards, a type of crack-layer formation also occurred towards the middle of the bed particles. This growth continued, even though the layer growth outwards stopped. Even though the mechanism does not directly relate to agglomeration per se, it will result in fragments sticking to the furnace wall, causing slagging. Preventing the formation of melt, thus hindering agglomeration, would also slow down the crack-layer formation. Crack-layer formation was first noted by Brus et al. (2005) and further investigated by He et al. (2017), who put forward a time-dependent mechanism explaining the phenomenon. This framework can be seen in Figure 6, from the initial coating build-up progressing to crack formation and ultimately breaking down the bed particles. According to He et al. (2017), gaseous alkali compounds, mainly K, diffuse through cracks in the coating, and the crack formation continues inwards and attacks the quartz particle. The diffusion proceeds over time, both widening and deepening the cracks. Finally, necks between the cracks start forming on particles. The formation of necks is what finally could lead to a breakdown of the initial bed particle.

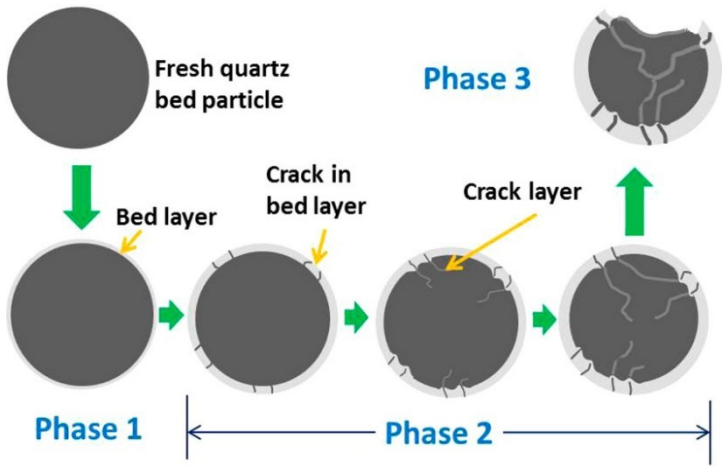

Figure 6 The proposed mechanisms for crack layer formation are presented in a schematic view (He et al., 2017).

3.2 Melt-induced agglomeration

In contrast to coating-induced agglomeration, where the melt is formed due to reactions between the bed material and the ash, melt-induced agglomeration stems from the fuel ash itself. In the case of melt-induced agglomeration, the composition of the ash is such that a molten phase can be formed from the ash itself. The naming in itself is somewhat misleading, since both types of agglomeration related to ash require a molten phase. The melt-induced mechanism is often associated with herbaceous fuels where the main common denominator is a relatively high concentration of silica, with examples such as wheat straw and rice straw (J. D. Morris et al., 2018). The coating described in the previous section is usually absent in melt-induced agglomeration. Moreover, the wetting of the bed particle is limited, and the glue resembles the global ash composition of the fuel.

In addition, two sub-mechanisms have been put forth, as shown in Figure 7. On the left, agglomerates start forming around a fuel particle, in the example, a pellet. The bed particles adhere to the surface of the fuel particle onto molten ash. As the combustion proceeds and the fuel particle is charred and finally completely combusted, the resulting agglomerate is hollow and fuel shaped. The burning fuel particles also created localized hot spots in the

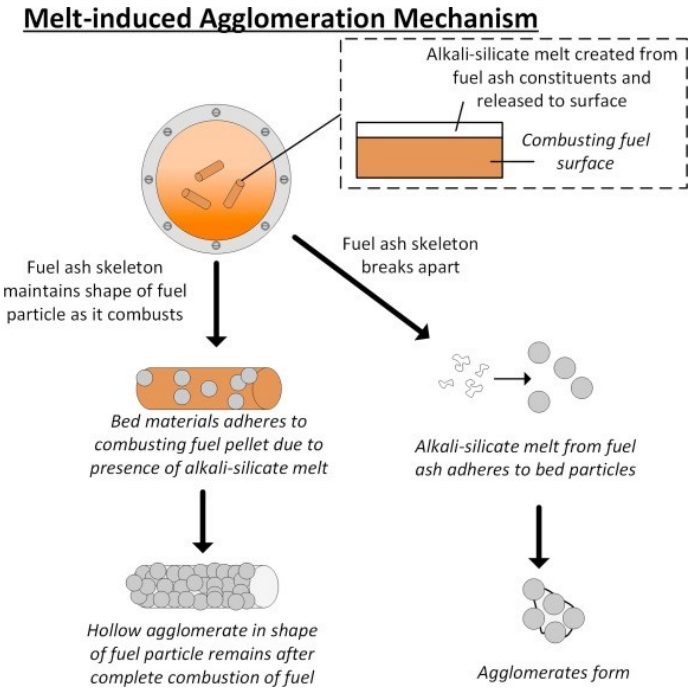

Figure 7 The two reaction paths associated with melt-induced agglomeration (Morris et al., 2018).

bed, enhancing the presented effect. Individual molten ash particles that have broken off from the fuel could also start the propagation of an agglomerate with the bed particles adhering to the ash. This is represented in the figure on the right-hand side (J. D. Morris et al., 2018).

3.3 Prevention of bed agglomeration

As is evident from the previous chapter, agglomeration is inevitable when combusting problematic biomass in FBC. When considering the problem at a plant scale, the optimization should be seen in relation to steam production, which is often the end goal. There is a vast number of process parameters that can be adjusted in a boiler which could be categorized into inputs, such as fuel and bed material, and process conditions, such as bed temperature and gas velocity of the fluidization media. Changes in operational parameters can also cause chain reactions, which makes it more difficult to predict the behavior and take corrective measures. A brief overview of the most important influencing parameters will be given in this section.

3.3.1 Operational changes

There is an extensive amount of reports in the literature focusing on the influence of temperature on agglomeration. The agglomeration tendency is directly related to the bed temperature, as shown by Lin et al. (2003) and Chirone et al. (2006). A higher temperature increases the melt fraction in the bed but also its viscosity, which makes it easier to wet bed particles and, thus, induces agglomeration (Gatternig and Karl, 2015). Modeling done by He et al. (2016) suggests a 2-3 times increase in layer growth rate when increasing the bed temperature from 850 to 900 °C. The amount of melt needed for agglomeration is hence achieved significantly faster. From an economic point of view, lowering the bed temperature is due to lower steam yields (Leckner, 2016).

The velocity of the fluidization gas, U, is an essential parameter in an FBC boiler. U / U_{mf}, or the ratio of the fluidization gas velocity to the minimum fluidization velocity, which is called the fluidization number, has a solid correlation to agglomeration (J. D. Morris et al., 2018). Doubling U resulted in a 30% increase in operational time before agglomeration. The effect can be explained by an increase in particle velocity, which subsequently, increases the force

required to propagate the formation of agglomerates. In addition, it results in better mixing and more even fluidization (Lin et al., 2003).

3.3.2 Fuel

As previously described in this thesis, the ash-forming elements in the fuel and their behavior during combustion play a significant role in agglomeration. Alkaline earth metals and alkali within the fuel are the main culprits in this aspect. Gatternig and Karl (2014) state that fuel is one of the most important factors to consider.

Co-firing of different biomasses might present a practical solution with several benefits and could offer solutions for fouling, corrosion, and agglomeration (Hupa, 2005). Rape seed cake, a high P-fuel blended with bark, is effective in mitigating agglomeration (Piotrowska et al., 2012). Silvennoinen and Hedman (2013) studied co-firing of agricultural waste and wood chips in a full-scale BFB. The used waste fuels were sunflower seed hull pellets and oat. The bed was operated below 750 °C. The trial was successful, demonstrating that up to 30% of blended agrofuels could be used.

Pre-treatments have been studied as a measure of preventing agglomeration, most notably leaching with water. Wu et al. (2019) leached wheat straw with water, and it resulted in a 26% decrease in the ash-forming matter and consequently increased the melting temperature of the ash. Potassium decreased significantly, which should improve agglomeration-related problems. The authors did not, however, do any combustion tests nor discuss the economic implication of treating the resulting wastewater.

Gatternig and Karl (2015) note that the density of the fuels might have an impact on agglomeration, naming wheat straw as an example. The presented effect is omitted to the possibility that fuels with a low density might stay afloat on the fluidized bed. Since the floating fuel is not submerged, the heat transfer is lower, increasing the temperature and thus promoting agglomeration.

3.3.3 Bed material

Quartz plays a central role in coating-induced agglomeration, as natural sand, a quartz-based material, is presently the most used bed material. The main reason for it is both availability and price. When considering agglomeration, it is, however, a suboptimal

solution, as Si plays a central role in the coating-induced agglomeration. Alternative bed materials have been studied extensively, with a focus on quartz-free alternatives. Explored alternatives include blast furnace slag, olivine, diabase, ilmenite, and bauxite. The studied material contains mainly Al, Mg, Ca, and Fe in different compounds and have been shown to reduce agglomeration (Morris et al., 2018). This is, however, not the case for fuels that result in melt-induced agglomeration, as Si is available in the fuel itself (Grimm et al., 2011). Mixing bed material has been presented as an option to mitigate the economic implications of using more costly materials. A mixture of bauxite and silica sand has been shown to decrease agglomeration, while a mixture of silica sand and $CaCO_3$ eliminated agglomeration (Knutsson et al., 2014).

Active replacement of the bed material during operation provides an option for preventing agglomeration while still using natural sand. There are some associated drawbacks, such as the cost of replacement and heat loss (Bartels et al., 2009).

3.3.4 Additives

Altering the available chemical reactants can be achieved by additives. The aim is to shift the equilibrium in the bed and inhibit or delay the formation of the sticky molten phase that causes agglomeration. The additives can be introduced with the fuels, either directly or mixed into a pellet or directly into the furnace (Morris et al., 2018).

Steenari et al. (2009) conducted ash sintering experiments with three additives: kaolinite, limestone, and sodium bicarbonate ($NaHCO_3$), with several different fuels. The two former additives showed excellent performance in reducing agglomeration. Kaolinite mainly consists of kaolinite, $Al_2Si_2O_5(OH)_4$, which reacts to meta-kaolinite $Al_2Si_2O_7$ at 500-800°C (Wang et al., 2011). The effect of kaolinite is attributed to the capture of K, which reacts with kaolin to form $KAlSiO_4$ and $KAlSiO_6$ $KAlSi_2O_6$ (Steenari et al., 2009). An example of the reaction of capturing alkali with kaolinite is shown below:

$$Al_2O_3 \cdot 2SiO_2(s) + 2\,KCl(g) + H_2O\,(g) \rightarrow KAlSiO_4(s) + 2HCl(g) \qquad (7)$$

The effect of limestone, $CaCO_3$, as an additive in CFB-boiler has also been tested. It showed promising results for mitigating agglomeration in the case of phosphorus-rich fuels. Calcium was shown to react with K and P, forming silicates with higher melting points as well as

forming a protective layer inhibiting the formation of low-melting silicates altogether (Barišić et al., 2008).

Öhman and Nordin (2000) tested kaolinite as an additive. They mixed ten wt-% into the bed of silica sand. The trials were conducted in a lab-scale BFB with bark and wheat straw as fuels. The furnace was heated until agglomeration occurred, and both cases showed an increase in temperature. Morris (2021) conducted experiments in a 65 kW_{th} boiler with kaolinite and dolomite additives in the bed. The results were promising in the case of miscanthus as fuels, whereas there was little to no improvement with wheat straw as a fuel.

The effects of additives are indisputable and have been proven effective. The addition of Ca, Mg, and Al in different combinations can mitigate agglomeration. As with alternative bed materials, the effect is more pronounced in the case of coating-induced agglomeration. The literature, however, seldom discusses minimum viable additive dosage leaving some questions unanswered.

4 Experimental

A set of experiments were conducted to investigate the inhibiting effect of additives on bed agglomeration. Two fuels, sunflower seed shells, SFSS, and wheat straw, along with two additives, limestone and kaolinite, were chosen for the experiments. The experimental matrix of the campaign can be seen in Table 1. The total weight of the bed was 375 g in every experiment. The additives were mixed with quartz into the bed, and the amounts are indicated by wt-% of the total bed. The experiments were performed at three different temperatures, 800, 850, and 900°C.

Table 1 The experimental matrix in this study.

Fuel	**Bed**			**Temp (°C)**
	Quartz sand (wt-%)	Kaolinite (wt-%)	Limestone (wt-%)	
SFSS	100	-	-	800
SFSS	100	-	-	850
SFSS	100	-	-	900
SFSS	98.7	1.3	-	850
SFSS	97.5	2.5	-	850
SFSS	95	5	-	850
SFSS	95	-	5	850
Straw	100	-	-	800
Straw	100	-	-	850
Straw	100	-	-	900
Straw	95	5	-	850
Straw	90	10	-	850
Straw	95	-	5	850

In the following sections, the experimental setup used, the fuels and additives, and the consequent analysis of the samples are presented. Some of the related challenges will also be discussed, mainly relating to the equipment.

4.1 Laboratory-scale fluidized bed reactor

All the experiments were performed in a lab-scale BFB boiler developed and used in several studies at ÅAU (Sevonius et al., 2014, 2019, 2020; Zevenhoven et al., 2018). Figure 8 shows a schematic overview of the reactor and the different parts. The reactor can be divided into three sections: a preheater, a combustion section, and an exhaust and instrumental section. The reactor is approximately 1.5 m high. The reactor is made of a 4 mm thick AISI 316 steel pipes with an outer diameter of 110 mm and an inner diameter of 90 mm. The sections are connected with flanges, which allows dismantling for cleaning and collection of samples after each experiment. Both the preheater and combustion section is heated with an electric tube furnace, allowing for even conditions in the furnace. The fluidizing air is fed from the bottom of the preheater through a perforated pipe and heated by the preheater walls. The air passes through a 150-mesh steel net into the combustion section and fluidizes the bed. The fuel is fed into the reactor with a screw feeder connected to the main reactor tube above the bed.

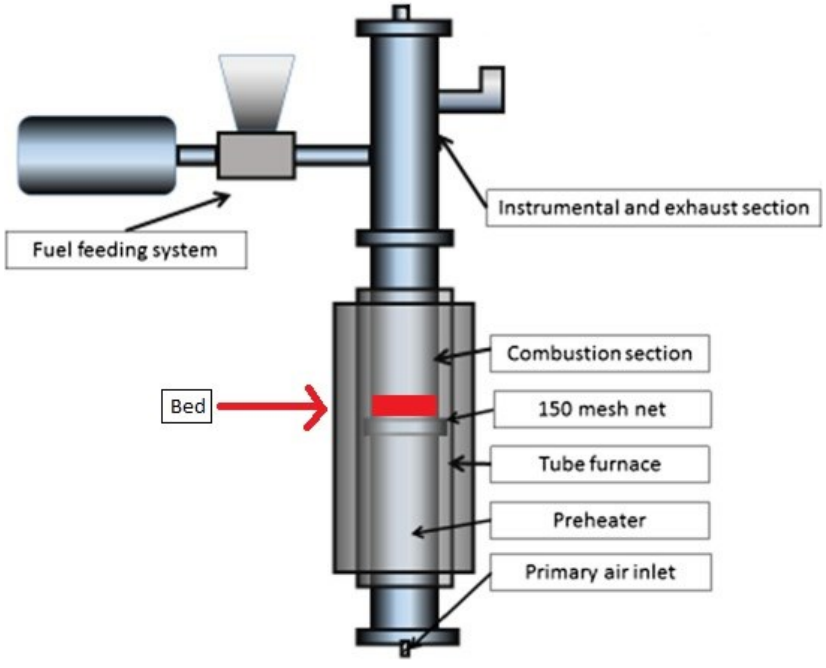

Figure 8 A schematic overview of the reactor used in the experiments (Sevonius et al., 2019).

Two indicators were used to detect defluidization: pressure drop over the bed and temperature differences in the bed. Thermocouples were positioned 3 and 7 cm above the mesh net holding the bed, additionally one in the preheater and one in the upper part of the exhaust section. The assembled reactor can be seen in Figure 9.

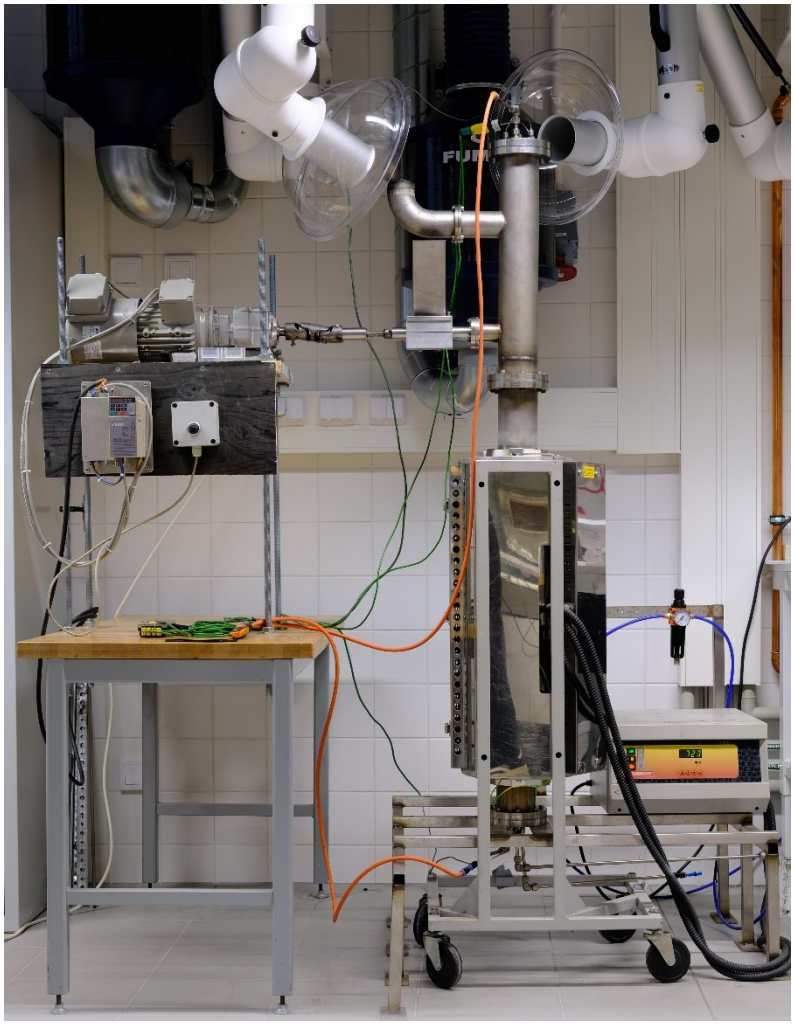

Figure 9 The lab-scale fluidized bed reactor pictured in the lab fully assembled. External systems such as the electric motor for fuel feed screw and fume suction are visible.

4.2 Agglomeration experiments with fluidized bed reactor

The reactor was loaded with the bed material and assembled before heating the reactor. The fluidization medium, air (10 Nl/min), was turned on when the target temperature was reached. After a short time, when a steady state was reached, the experiment was started. When the fuel feeding was started and the combustion initiated, the oven temperature had to be adjusted to keep the reactor at the target temperature. The bed was maintained at

approximately ±10 °C from the set temperature for the experiment. Adjustments were either made by stopping the addition of fuel for a certain time or by adjusting the heating of the oven. During some of the experiments, the fuel-feeding screw was severely fouled, which affected the feeding rate. In those cases, the frequency of the motor had to be adjusted to maintain the fuel feed rate. The experiments were run until defluidization occurred or the amount of fuel fed to the reactor reached 500 g.

Two indicators were used to detect defluidization: pressure drop over the bed and temperature differences in the bed. The two thermocouples positioned in the bed were used for this purpose (3 and 7 cm above the mesh net holding the bed). The pressure drop measurements were taken from the preheater and the top of the combustion section.

When the bed is defluidized, an immediate decrease in the pressure drop will occur. This is a result of channeling in the bed, which lets the air move more freely through the bed. Defluidization also leads to an increase in the temperature differences in the bed when the mixing becomes worse (Sevonius et al., 2014).

In some of the experiments with additives, white particles could be observed at the exhaust, indicating that a part of the additives was entrained in the exhaust gas. However, the amount seemed to be insignificant to the overall results.

4.3 Analysis of bed samples

After the experiments, the reactor was cooled down before dismantling and collecting samples from the bed material. Sintered particles were selected from the bed. Agglomerates were cast in epoxy, and to achieve a cross-section of the sand particles, the epoxy castings were polished. To retain alkali species from dissolving, kerosene oil was used during polishing. The samples were periodically checked with an optical microscope during polishing to determine their status. After the polishing, the samples were cleaned using petroleum ether in an ultra-sonic bath. The residual oil was extracted in a vacuum. The samples were coated with a thin layer of carbon to make the samples electrically conductive and hence avoid surface charges. A strip of carbon tape was also added to the rim of the samples. The cross-sections were analyzed by means of scanning electron microscopy, SEM, and energy-dispersive x-ray spectroscopy, EDS.

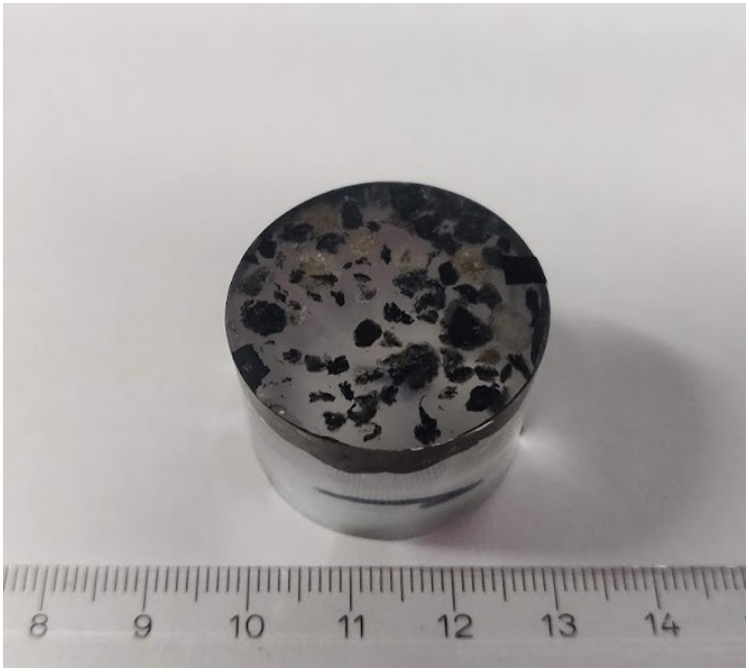

Figure 10 Agglomerates cast in resin and prepared for SEM/EDS. Polished in to expose cross-section and coated with a thin layer of carbon. Conductive tape was applied around the side to further improve conductivity.

4.4 FuelsTable 2 shows the composition of the two fuels used in the experiments. The fuels were selected based on the agglomeration mechanisms they exhibit. Both fuels represent agricultural waste fuels. However, their composition varies relatively much, which indicates a differing behavior. Sunflower seed shells, SFSS, are expected to result in coating-induced agglomeration based on literature (Tropp, 2020). It has an ash content of 3.0 wt-%, with the main ash-forming element being K. Straw is expected to result in melting-induced agglomeration based on literature (Brus et al., 2005). It has 9.4 wt-% of ash. Relative to SFSS, it has a significant amount of Si, and it also has significant amounts of alkali metals. The fuels were received as pellets, which were lightly ground to make them compatible with the lab-scale reactor. Since both fuels had been made into pellets and stored indoors, they had relatively low moisture content.

Table 2Table 2 shows the composition of the two fuels used in the experiments. The fuels were selected based on the agglomeration mechanisms they exhibit. Both fuels represent agricultural waste fuels. However, their composition varies relatively much, which indicates a differing behavior. Sunflower seed shells, SFSS, are expected to result in coating-induced agglomeration based on literature (Tropp, 2020). It has an ash content of 3.0 wt-%, with the main ash-forming element being K. Straw is expected to result in melting-induced

agglomeration based on literature (Brus et al., 2005). It has 9.4 wt-% of ash. Relative to SFSS, it has a significant amount of Si, and it also has significant amounts of alkali metals. The fuels were received as pellets, which were lightly ground to make them compatible with the lab-scale reactor. Since both fuels had been made into pellets and stored indoors, they had relatively low moisture content.

Table 2 The compositions of the two fuels that were used in the experiments. LHV and HHV denote lower and higher heating values, respectively.

Analysis	Wheat straw	Sunflower seed hulls
Volatiles (wt−%)	62.3	64.7
Moisture (wt−%)	13.1	15.5
Ash, 550 °C (wt−% of dry matter)	9.4	3
HHV, wet (MJ/kg)	17.7	20.5
LHV, dry (MJ/kg)	14	15.9
Elemental composition, wt−% of dry solids		
C	44.0	50.9
H	5.98	6.18
N	0.86	0.80
O	39.7	38.9
S	0.12	0.14
Cl	0.38	0.04
Ash-forming elements, mg/kg of dry solids		
Si	24684	266
Al	1032	47
Fe	624	90
Ca	5410	3023
Mg	1128	1761
Na	486	22
K	10875	8468
P	1056	751
Ti	59	3
Mn	42	7

4.5 Bed material and additives

Quartz sand (250–300 µm) was used as bed material in the experiments. The additives were mixed into the bed material before the reactor was assembled. Limestone was obtained as rocks in a size range of 2–4 cm, which then was ground and subsequently sieved to 125 < x < 500 µm. The limestone originated from a quarry in Gotland, Sweden. The kaolinite was obtained as pressed granules that contained some residual moisture. The particles were dried at 105 °C for 24h before sieving them to a similar size as the limestone. The effects and properties of these additives were discussed more in detail in Section 3.3.4

5 Results and discussion

The results of the experimental campaign will be presented in this chapter. Firstly, some general comments regarding the experiments and the equipment will be discussed. The results are presented in **Error! Reference source not found.**–6 and Figures 11–21, with a division based on the fuel. The reason for each shutdown is also included in the tables, as there was a set amount of maximum fuel-fed (500 g) before the planned shutdown. The limit amount of fed fuel was set to 500 g to be able to do one test during working hours and safely shut down the equipment before the end of the day.

The tests can be compared based on the fed amount of fuel, the used additive, as well as the test temperature. The temperature indicated in the tables was the target temperature. In practice, they fluctuated over time and were within +- 10 °C. The amount of alkali is calculated from the fed fuel amount and fuel analyses. It is, however, unknown to which extent the alkali stays in bed and how much is vaporized. Lin (2003) showed that most of the K fed remains in the bed at temperatures below 900 °C. The conclusions were drawn from experiments firing straw pellets in a similar reactor to the one used in this thesis. The accumulation of K in the bed was linear even though it was somewhat lower than the calculated theoretical amount. The applicability of these findings is, however, questionable, and it can be assumed that alkali escapes the bed at least partly. It would have to be validated in longer tests in order to make assumptions about the behavior in full-scale boilers. Potassium escaping the bed would have a positive effect on agglomeration but would affect the process downstream.

In addition to the fuel amount, the formed agglomerates and the remaining bed material were compared. The comparison was made both by qualitative and quantitative measures. Composition, type, and extent of coatings were observed and compared with the help of SEM/EDS images and elemental analyses.

5.1 Defluidization experiments

After each defluidization experiment, the reactor experienced some fouling in the upper combustion section and exhaust area. The amount was highly influenced by the length of the experiment and the fuel. In the experiments with additives, white particles could be observed at the exhaust. This would imply that some amount of the additive becomes entrained in the flue gases. In order to determine that the amount was insignificant, the reactor was heated up with bed material and additive to 850 °C. At that point, the fluidization air was turned on for 30 min. After cooling, the bed was weighed to confirm that the bed material remained in place. The main challenge that primarily affected the longer runs was the plugging of the fuel screw feeder. Additionally, in some experiments, the temperature fluctuations were more significant. Figure 11 shows two different experiments with SFSS, one shutdown due to defluidization (a) and one with a planned shutdown (b). The electrical furnace is regulated by the thermocouple denoted T1, which

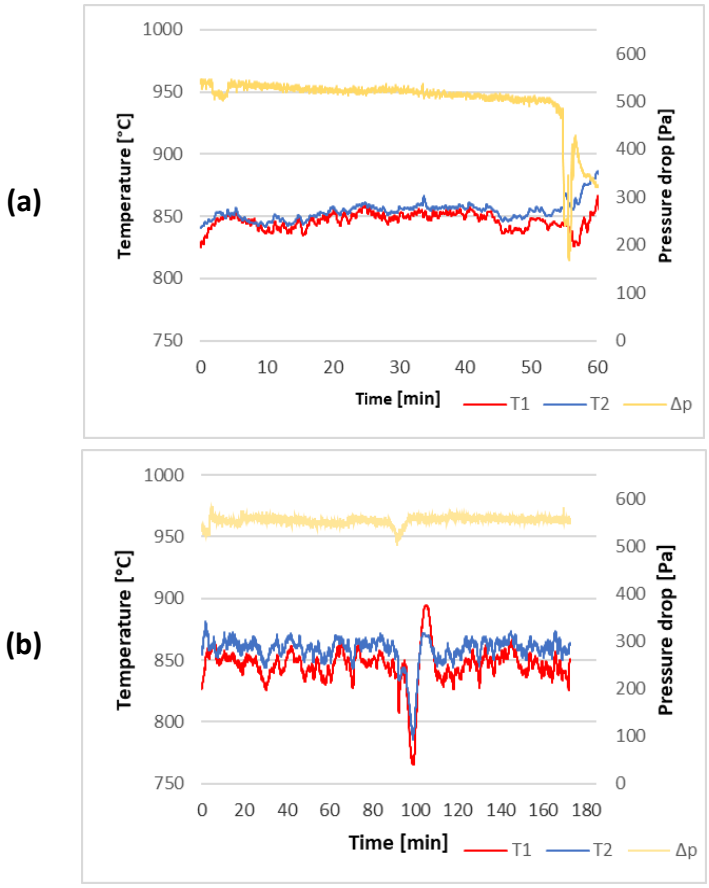

Figure 11 Temperature and pressure data from two different tests with SFSS at 850 °C. A test (a) without additives ended in defluidization, and a test (b) with 5% kaolin resulted in a planned shutdown.

is located inside the bed. T2 denotes the temperature just above the bed. In (b), the temperatures fluctuate during the whole test, especially at around 100 minutes. These fluctuations can be attributed to problems with fuel feeding.

5.2 Sunflower seeds husks

An overview of the results obtained with sunflower seed husks can be seen in **Error! Reference source not found.**. The numbers in the table refer to the amounts at the end of each experiment, except for the temperatures, which refer to the whole duration of the test. The table lists the additive used, the temperature for the experiment, the total amount of fuel fed during the test, wt-% K in the bed at the end of the test, the reason

Table 3 Test results from the experiments with sunflower seed husks

Additive	Temperature [°C]	Fuel fed [g, a.r.]	Additive in bed (wt-%)	K in bed (wt-%)	Additive / K (mol/mol)	Shutdown reason
-	800	501	-	0.97%	-	Defluidization
-	850	118*	-	0.23%	-	Defluidization
-	900	49	-	0.09%	-	Defluidization
Kaolin	850	381	1.35%	0.73%	0.3	Defluidization
Kaolin	850	503	2.5%	0.97%	0.4	Planned
Kaolin	850	557	5%	1.07%	0.7	Planned
Limestone	850	139	5%	0.27%	-	Defluidization

*Base test case, experiment was repeated three times, and the result indicates the average result.

for the shutdown, and the molar ratio of K to additive. Overall, the experiments progressed well.

The impact of temperature was significant as 501 g of fuel was fed at 800 °C without defluidization, and only 118 g could be fed at 850 °C before the test ended in defluidization. Some agglomerates could be found in the test conducted at 800 °C but to a limited degree. The pressure difference decreased during the experiment, pointing to some agglomeration proceeding. The effect of a lower temperature on agglomeration has also previously been shown in several studies (Lin et al., 2003; Scala and Chirone, 2008). The data also corresponds with a model developed by He (2016), suggesting a 2-3 decrease in terms of fuel that could be fed from tests done at 850 °C to 900 °C.

Figure 12 shows a representative agglomerate formed when burning SFSS. The table next to the image shows the compositional analysis conducted with EDS for different points. Precise neck formation and the initial coating of the quartz particles can be seen. The neck area almost exclusively consists of Si and K with no apparent variation depending on the position. Point 1 indicates a reference point for analyzing the quartz particle. The minor amount of K is most likely a contaminant. The coating on particles is in the range of 1–3 µm, whereas the necks are 15–85 µm. The coating layer and composition are typical for coating-induced agglomeration. When handling the bed material while

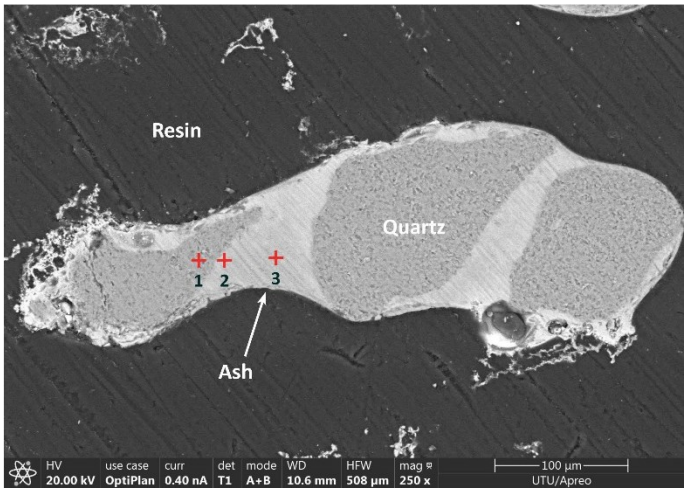

	1 [at-%]	2 [at-%]	3 [at-%]
Si	99.4	70.4	69.4
K	0.6	29.6	29.5
Ca	0	0	0
Al	0	0	0.8
S	0	0	0.3

Figure 12 Image of a typical agglomerate firing SFSS, in this case at 850 °C without additives. Necks between the quartz particles and a coating surrounding quartz particles can be observed. Locations marked 1–3 represent the EDS analyses given in the adjoining table on an O-free basis.

retrieving samples, many agglomerates were relatively fragile and fell apart while handling them. The agglomerates were mainly of a diameter of approximately 0.5–1 mm.

5.2.1 Effects of kaolinite

The tests with kaolinite resulted in a significant reduction of bed agglomeration tendencies when burning SFSS. With a dosage of 2.5 wt-% and 5 wt-% of the bed, the experiment was ended before defluidization. Only a few agglomerates could be observed when inspecting the bed material during retrieval. In addition, it could be concluded that the structure of the few formed agglomerates was different from that of the test without kaolinite. The structure was less dense and tended to break easily during collection. For experiments with 2.5 wt-% and 5 wt-% of the bed, only individual bed particles could be collected. A dosage of 1.35 wt-% kaolinite in the bed improved performance compared

to the base case from 118 g to 381 g of fuel. Figure 13 shows the relationship between the amount of fuel fed, wt-% kaolinite in the bed (secondary y-axis), and the molar ratio of kaolinite to K (secondary y-axis) for three experiments.

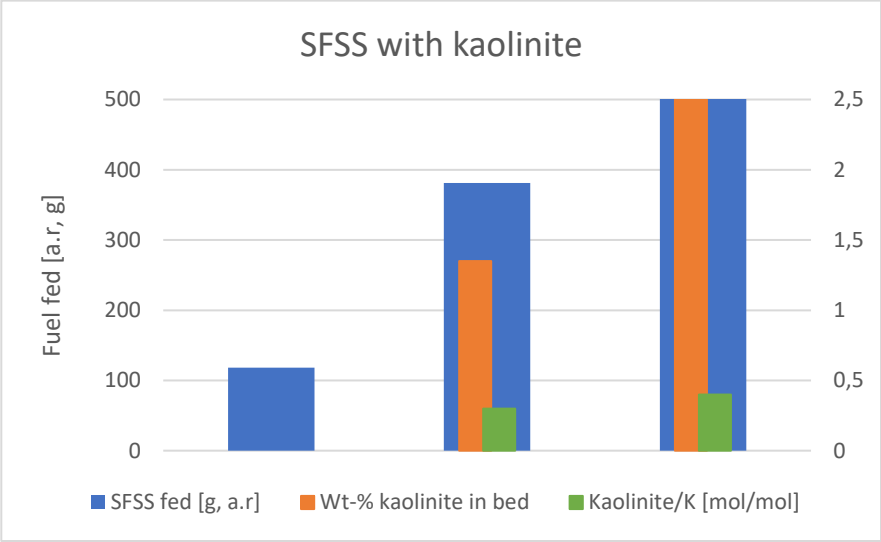

Figure 13 Test results firing SFSS (from left) with no kaolinite, 1.25 wt-% kaolinite, and 2.5 wt-% kaolinite as an additive in the bed.

Figure 14 shows bed material retrieved from the experiment with 2.5 wt-% kaolinite of the bed, as practically no agglomerates were formed in the bed. Kaolinite particles are distinct from quartz particles. They are darker in color and appear to have a porous structure. Notably, no coating of particles can be seen, which indicates that K present in fuel ends up elsewhere. Analysis at point 1 gives distinct evidence of K absorption in

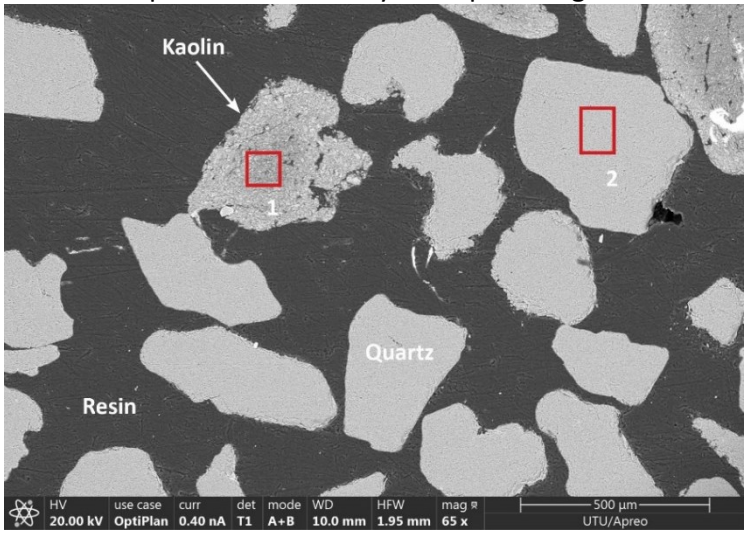

	1 [at-%]	2 [at-%]
Si	48.7	100
K	10.6	-
Al	48.7	-
Fe	0.6	-
Mg	0.4	-

Figure 14 Image taken of a bed sample collected from the experiment with 2.5 wt-% kaolinite as an additive in the bed. The test ended in a planned shutdown. Individual quartz and kaolin particles are visible. The locations marked 1–2 represent the EDS analyses given in the adjoining table on an O-free basis.

kaolinite with good penetration inwards of the particle. 10.6 at-% K on O-free basis was observed.

Figure 15 shows an agglomerate sample retrieved from the experiment with 1.35 wt-% kaolinite of the bed. The agglomerates were quite fragile and “fluffy” with a less dense structure compared to tests without additives. Both the quartz particles, here darker, and the kaolinite particles, lighter and porous, can be seen clearly. Individual particles, particles with a coating, and agglomerates can be observed. Kaolinite particles have formed agglomerates with quartz particles. Compared to tests with 2.5 wt-% kaolinite of the bed, the amount of K found in kaolinite is more than double in spot 4 (10.6 at-% vs. 28.2 at-%). The proportion of Al to K is almost 1 in point 4. If the reaction between K and

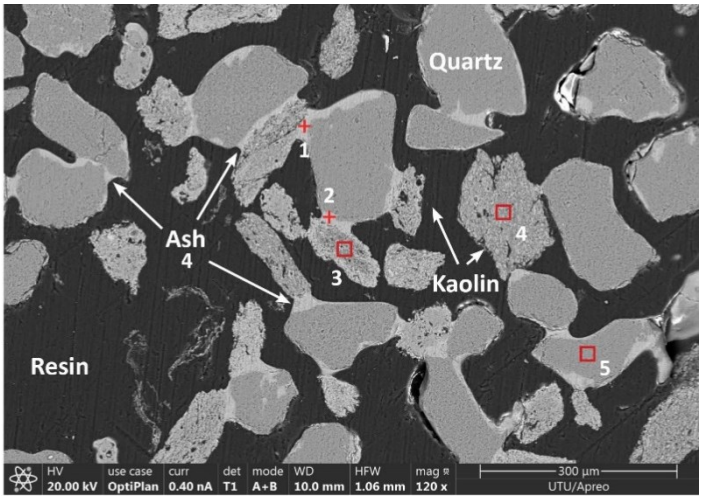

	1	2	3	4	5
	[atomic-%]				
Si	71.9	71.6	45.8	38.3	100
K	27.1	25.1	17.6	28.2	-
Ca	1.0	1.9	0.0	0.0	-
Al	-	0.4	36.0	33.2	-
Fe	-	-	0.7	0.3	-
Mg	-	1.0	-	-	-

Figure 15 Image taken of bed sample collected from an experiment with 1.35% kaolinite as additive. The test ended in defluidization. Clearly formed necks and agglomerates, as well as some coating of particles, is visible. Locations marked 1–5 represent the EDS analyses given in the adjoining table on an O-free basis.

kaolin is stoichiometric, this would indicate that the kaolin particle is saturated with K.

The EDS analyses point at the underlying mechanism of agglomerations mitigation by kaolinite. K is absorbed into kaolinite, thus inhibiting reaction with Si and limiting the formation of molten K-Si-silicate. There is no evidence of Al movement out of kaolinite particles, as can be seen in points 1 and 2. Some Ca is also present in the adjoining necks area; this might be a result of more extended experiments. No Ca could be observed in the tests without kaolinite which was significantly shorter. Previous work (He et al., 2014; Nuutinen et al., 2004) has indicated the movement of Ca towards the melt after its initial formation.

5.2.2 Effects of limestone

The experiments with limestone proved troublesome. Figure 16 shows the collected data from a successful experiment with 5 wt-% limestone in the bed. The bed was defluidized after 138 g of fuel had been fed to the reactor, a slight improvement over 118 g without additives. As indicated by the pressure difference data in the figure, a sudden drop indicating defluidization occurred shortly after the feed of fuel started. The fuel feeding was stopped, and the fluidization recovered shortly after. Fuel feeding was re-started after the bed had stabilized, and the experiment could be continued. Limestone resulted in less stable process conditions. It was more difficult to keep a constant temperature. Some sudden spikes in pressure drop were also encountered after the initial start-up. A feasible explanation for the sudden defluidization at the start could be the recarbonation of the limestone. This might be possible as CO_2 increases in the reactor after the ignition of fuel resulting in a disturbance in the bed.

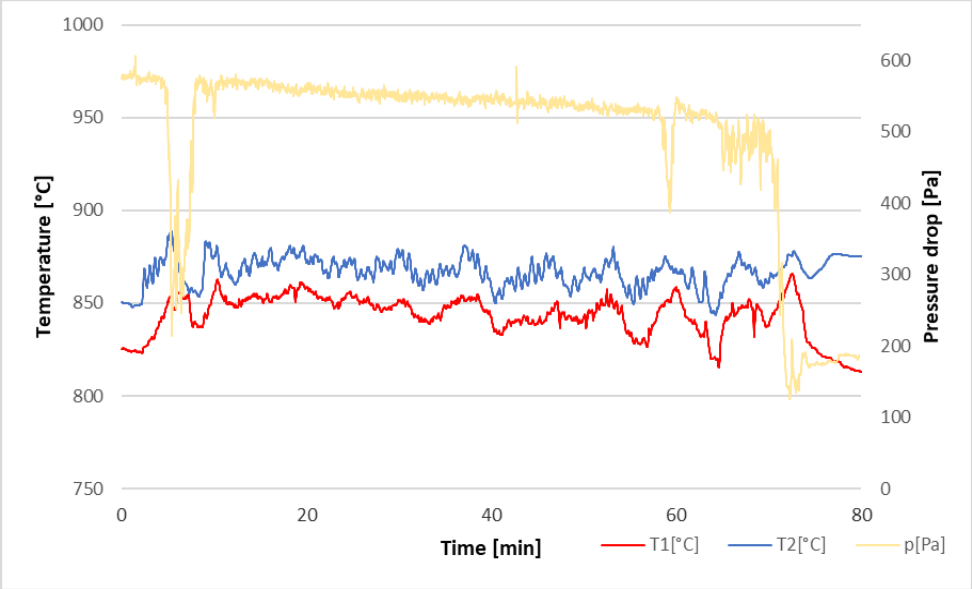

Figure 16 Temperature and pressure data from the experiment with limestone as additive and SFSS as fuel.

Figure 17 shows a bed sample taken from the experiment with 5 wt-% limestone in the bed. The coating can be observed on roughly half of the particles. Some agglomerates are also visible, with one limestone particle visible. The limestone particle is about 50–80 µm which would suggest that at least some fragmentation of the particles has happened. The darker shapes are quartz particles (point 2). The light layer around the

quartz particles and between the particles is ash (points 1 and 3). The limestone particle appears porous and is lighter than the quartz particles in the image (area 4 and point 5). As opposed to experiments without additives and with kaolinite, the composition of the ash deposits is different, and Mg, Al, S, and Fe can be observed (Figure 17 and Table 4). In the neck area (point 3) between a quartz particle and limestone, the composition also includes some Cr, which could be contaminants from the reactor walls. Point 5 appears interesting as the main component is Mg, with 44,2% in at-%. This is probably due to some impurities in the limestone, i.e., dolomite. The S found in points 1 and 5 probably originates from the fuel and has reacted with Ca to form $CaSO_4$. The constituents of the necks are still Si-K which attributes to the coating formation and sticking of bed particles to each other.

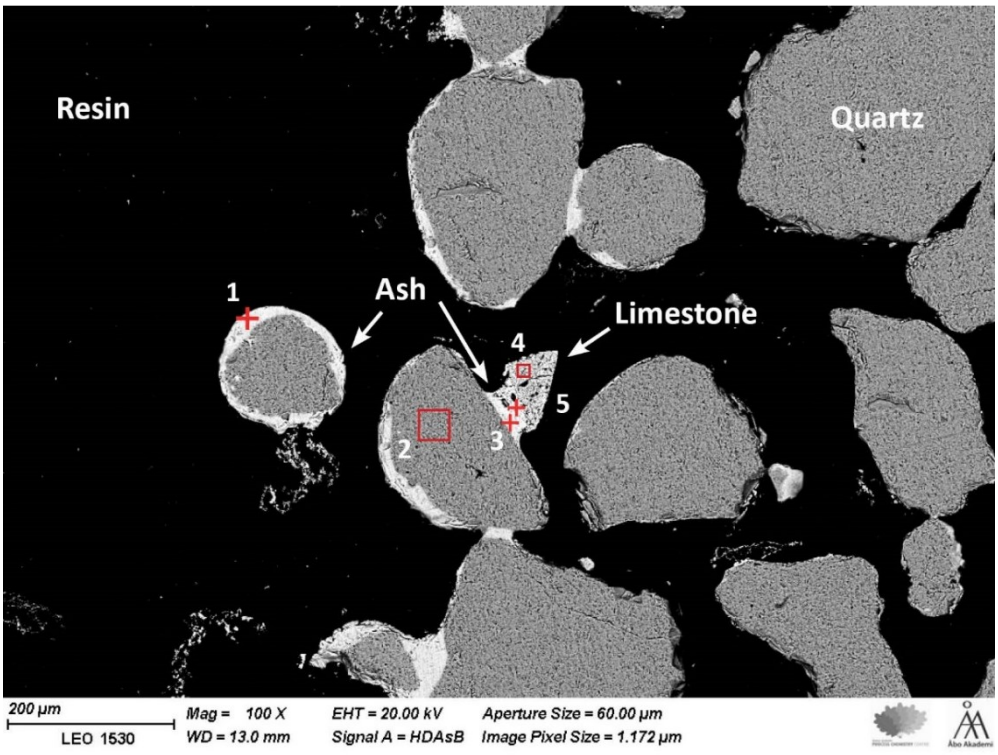

Figure 17 Image taken of a bed sample collected from an experiment with 5 wt-% limestone as additive in the bed. The test ended in defluidization. Formed necks and agglomerates, as well as some coated particles, are visible. The locations marked 1–5 represent the EDS analyses given in Table 4 on an O-free basis.

Table 4 EDS analyses results for the points marked 1 to 5 in Figure 17.

	1	2	3	4	5
			[atomic-%]		
Mg	2.2	-	2.1	0.6	44.3
Al	0.9	-	2.8	-	10.6
Si	61.2	100	61.3	0.2	12.6
S	1.1	-	-	-	0.5
K	24.9	-	24.5	0.1	0.8
Ca	7.2	-	3.0	71.0	31.2
Ti	-	-	0.5	-	0.8
Cr	-	-	0.2	-	0.3
Fe	0.4	-	5.4	-	4.3

5.3 Wheat straw

An overview of the results obtained with sunflower seed husks can be seen in Table 5. The numbers in the table refer to the amounts at the end of each experiment, except for the temperatures, which refer to the whole duration of the test. The table lists the used additive, temperature for the experiment, amount of fuel fed, wt-% K in the bed, the reason for the shutdown, and a molar ratio of K to additive by weight overall. Overall, the experiments progressed well, even though wheat straw was more troublesome from the viewpoint of agglomeration and fouling.

Table 5 Test result for wheat straw

Additive	Temperature	Fuel fed [g, a.r.]	Additive (wt-%)	K in bed (wt-%)	Additive / K (mol/mol)	Shutdown reason
-	800	87	-	0.22%	-	Defluidization
-	850	70*	-	0.18%	-	Defluidization
-	900	67	-	0.13%	-	Defluidization
Kaolin	850	325	5%	0.82%	0.9	Defluidization
Kaolin	850	426	10%	1.07%	1.8	Defluidization
Limestone	850	76**	5%	0.19%	-	Defluidization

*Base test case, experiment was repeated three times, and the result indicates the average result.
**Indecisive result with limestone, two different results were obtained, see section 5.3.2.

In comparison to SFSS, wheat straw performed distinctly worse, as also was predicted by the composition of the ash-forming elements, as a prior result presented in the literature. The base case resulted in defluidization after 70 g of fuel had been fed into the reactor as compared to 118 g for SFSS. Most of the formed agglomerates appeared to be formed around the remaining fuel char particles. Quartz particles had attached themselves to the surface of the char particles. Figure 18 shows a cross-section of an agglomerate formed around a char particle. These agglomerates were brittle, broke easily, and bed particles crumbled off during retrieval. Several studies (Lin et al., 2003; J. Morris, 2021; Visser et al., 2004) also report similar findings where agglomerates had formed around char particles and had a pellet-like structure in cases where whole pellets were used. Agglomerates forming around fuel particles is typical behavior for fuels promoting melt-induced agglomeration. Melt is formed from reactants within the fuel, which allows for the build-up of bed particles directly on the fuel particle.

In general, the reactor appeared to have more deposits and fouling after experiments with wheat straw as compared to SFSS. On some occasions, a layer of soot had started to build up in the bottom of the exhaust pipe. Wheat straw pellets were difficult to break down during fuel preparation and exhibited more fine particles after crushing. This could entail that more fines got entrained in the flue gases without reaching the bed, which appeared in the reactor as more fouling.

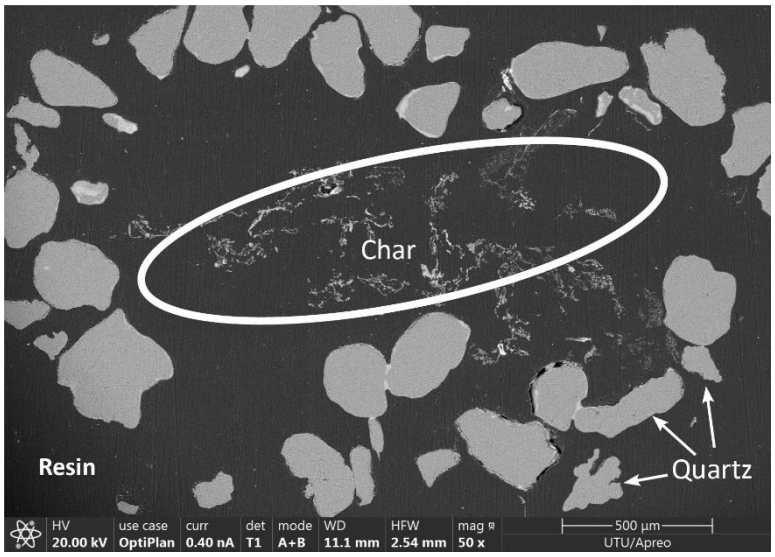

Figure 18 A SEM image showing a typical agglomerate that was formed when burning wheat straw. The core consisted of a char particle with bed material formed around the core.

5.3.1 Effects of kaolinite

The test with kaolinite and wheat straw resulted in a significant reduction of bed agglomeration. With a dosage of 5 wt-% and 10 wt-% of the bed, the fluidization behavior improved, although the experiments still ended in defluidization before the target of 500 g fed fuel was achieved. A dosage of 5 wt-% kaolinite of the bed increased the amount of fuel, which could be 70 g to 425 g of fuel. A dosage of 10 wt-% kaolinite of the bed further improved the performance as 425 g of fuel could be fed. The improvements were not proportional to the amount of kaolinite. Figure 19 shows the relationship between the amount of fuel fed, wt-% kaolinite (secondary y-axis) in the bed, and the molar ratio of kaolinite to K (secondary y-axis) for three experiments.

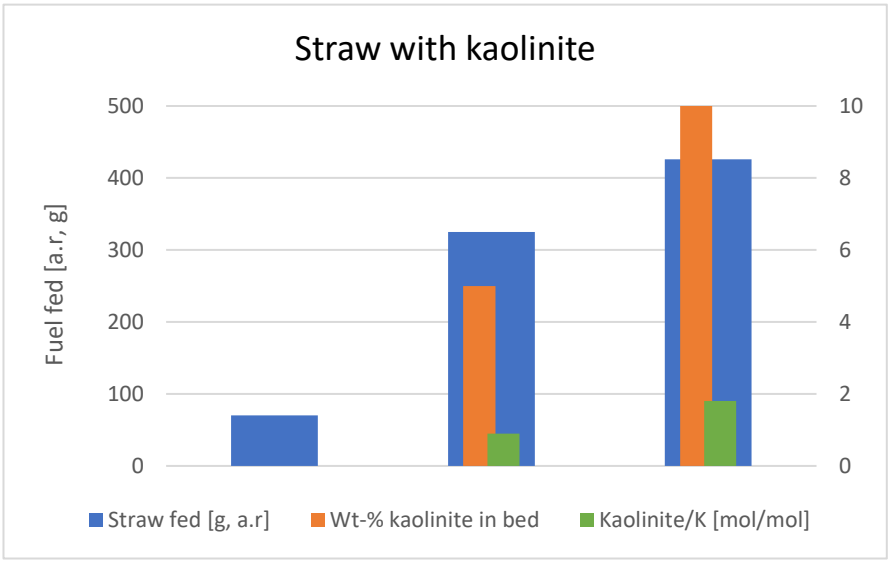

Figure 19 Test results firing straw (from left) with no kaolinite, 5 wt-% kaolinite, and 10 wt-% kaolinite as an additive in the bed.

Figure 20 shows a quartz particle (point 2) with some attached kaolinite particles (points 1 and 5). No coating on the quartz particle is visible other than where ash is attached. It is somewhat challenging to distinguish kaolinite from ash in the image, therefore the markings.

The analyses of point 1 and 5 indicate that the kaolinite particles have reacted with K. Some Na and Fe is also visible in the analyses, albeit in small amounts. Al to K molar ratio is close to 1. If the reaction between K and kaolin is stoichiometric, this would indicate that the kaolin particle is saturated with K. Phosphorus seems to be enriched in the

analyzed ash (points 3 and 4), with 24.2% and 15%, respectively, on an O-free basis in molar-%.

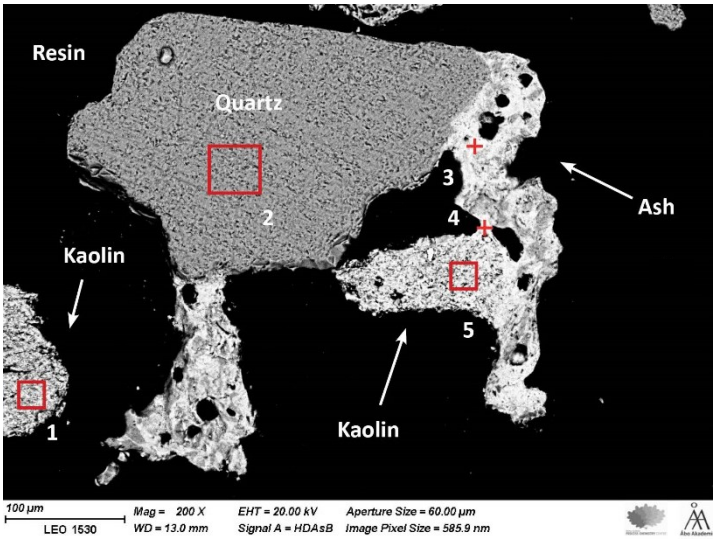

	1	2	3	4	5
	[atomic-%]				
Na	1.3	-	1.4	2.3	1.0
Mg	-	-	1.5	2.7	-
Al	33.4	-	0.2	-	32.5
Si	39.0	100	28.4	44.1	40.8
P	-	-	24.2	15.0	-
Cl	-	-	0.4	-	-
K	25.9	-	35.3	35.3	25.0
Fe	0.4	-	-	0.6	0.6
Ca	-	-	8.6	4.3	-

Figure 20 An image taken of an agglomerate collected from a wheat straw experiment with 5 wt-% kaolinite of the bed as additive. The test ended in defluidization. A quartz particle with attached kaolin particles as well as some fuel ash can be observed. The locations marked 1–5 represent the EDS analyses given in the adjoining table on an O-free basis.

Figure 21 shows a typical agglomerate as a result of melt-induced agglomeration, which is the case with straw as fuel. The elemental compositions of points 1 and 2 on the ash neck are similar. The main constituents are Si, K, and Ca. The distribution of the elements resembles that of the ash composition of the fuel. Overall, it should also be noted that practically no ash coating could be observed other than the connecting neck.

Kaolinite is less effective with straw than with SFSS. On a theoretical level, a kaolinite to K ratio of 0.5 should be sufficient to capture all K if the reaction between K and kaolin is stoichiometric. With a dosage of 5 wt-% of kaolinite in the bed, the ratio is 0.9, and with a ratio of 10 wt-%, the ratio is 1.8. The dosage is almost double the theoretical amount. As it is most likely that kaolinite reacts with gaseous species of K, probably, it does not come in contact with gaseous alkali to the same extent as with SFSS. This is a result of the close contact between the melt-forming elements which are already present in the fuel and its ash-forming matter. This is a result of the molten ash forming from the ash-forming matter itself. Some of the K does, however, come in contact with kaolinite as it is absorbed, as seen in the analyses shown in Figure 20.

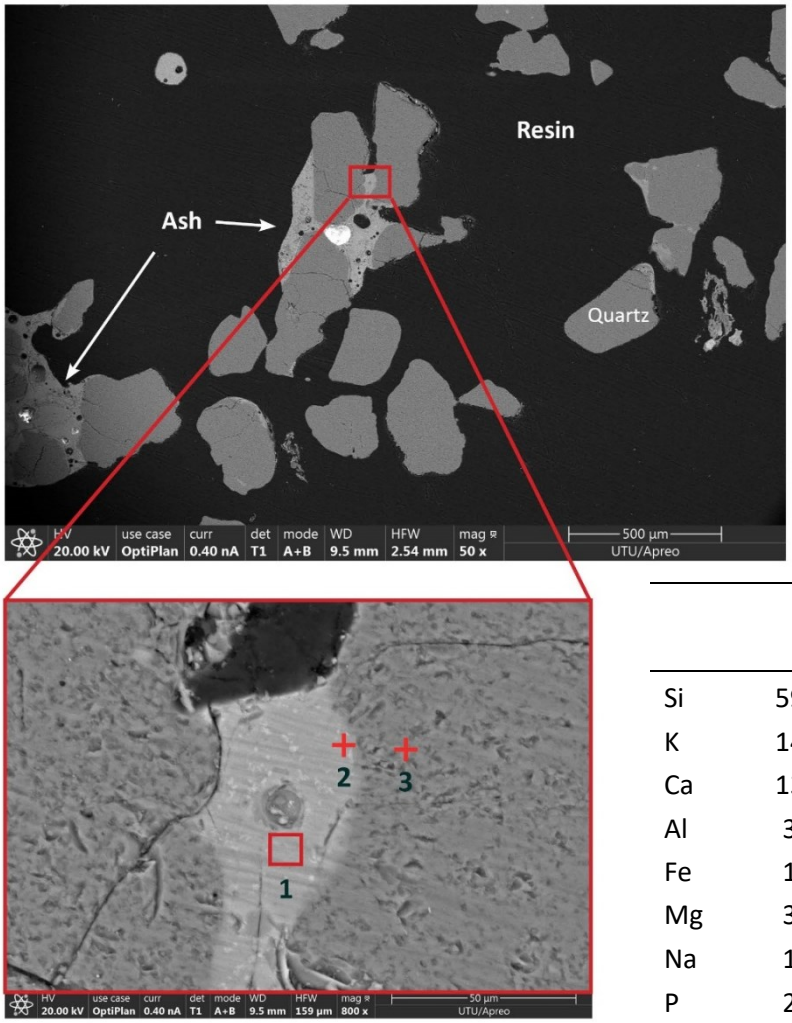

	1	2	3
		[at-%]	
Si	59.5	60.6	100
K	14.2	14.7	-
Ca	13.6	13.0	-
Al	3.2	2.7	-
Fe	1.5	0.9	-
Mg	3.9	4.4	-
Na	1.2	1.3	-
P	2.7	2.1	-
Ti	0.2	0.3	-

Figure 21 An image taken of an agglomerate collected from a straw experiment with 5 wt-% kaolin as an additive in the bed. The test ended in defluidization. A typical agglomerate can be seen in the middle, as well as a close-up of the neck. The locations marked 1–3 represent EDS analyses given in the adjoining table on an O-free basis.

5.3.2 Effects of limestone

Experiments with limestone proved troublesome, as their temperature was more difficult to control during the experiments. Figure 22 shows collected data from two different experiments with 5 wt-% limestone in the bed. The bed defluidized after 10 g of fuel in the first example (a) and 76 g of fed fuel in the second example (b). The dotted line indicates the start of fuel feeding and the dashed line defluidization of the reactor. The difference between the two experiments was a result of a malfunction of the equipment. In the case of b, the reactor was heated two times. The pressure metering device did not work, and the reactor was cooled in order to diagnose the problem. No fuel was fed after the first heating, nor was any bed material removed. The reactor was

heated the next day again, resulting in a successful experiment. The improvements over the base case without additives were only slight, 70 g vs. 76 g. The limestone probably calcined during the first heat-up period, thus altering the starting conditions.

Limestone resulted in less stable process conditions overall, which can be seen in Figure 22 as significant temperature fluctuations. The defluidization signal is not as evident in the second experiment (b). It was, however, concluded that the bed defluidized as the temperature difference between T1 and T2 grew to almost 100 °C.

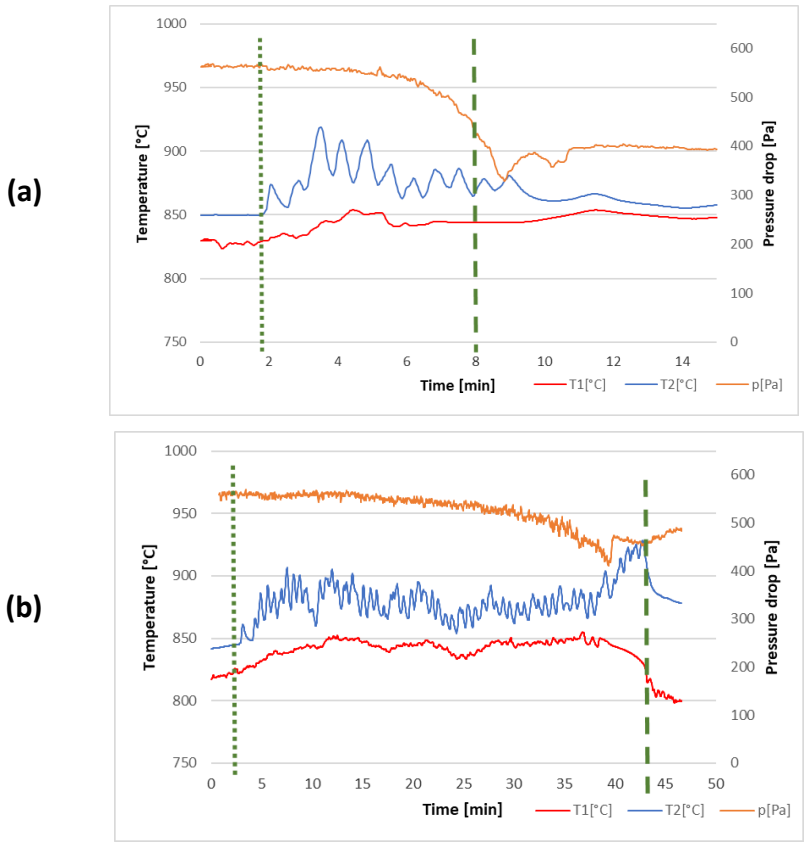

Figure 22 Temperature and pressure data from two different tests with straw and 5 wt-% limestone in the bed as additives. A test (a) shortly after the start of the experiment and b(b) a longer experiment. The dotted line indicates the start of fuel feeding, and the dashed line indicates defluidization.

The bed sampling from the experiment with 10 g fuel fed showed only some agglomerates but to a lesser extent compared to all other cases where defluidization occurred. It might be that the reactor was plugged by a dense layer forming on top of the bed, as it looked to have occurred upon visual inspection. No agglomerates could, however, be obtained as the structure crumbled when the reactor was disassembled.

Figure 23 shows an agglomerate from the experiment where 76 g of fuel was fed with five wt-% limestone in the bed as an additive. EDS analyses are given in Table 6. The most notable feature seen in the image is a uniform coating of the bed particles. It is typically a rare occurrence with wheat straw. This might be a result of the limestone in the bed providing Ca and thus altering the chemistry. However, no overall conclusions can be made from this single sample. One limestone particle can be seen in the image (points 3 and 5), with Ca being the most significant constituent. The two points (1 and 4) where ash has been analyzed vary a lot. For instance, Mg, Ca, and P are enriched in point 4, while point 1 has double the amount of K. Sulfur can be seen in both pints 3 and 4, which indicates that the limestone has reacted with S to form $CaSO_4$.

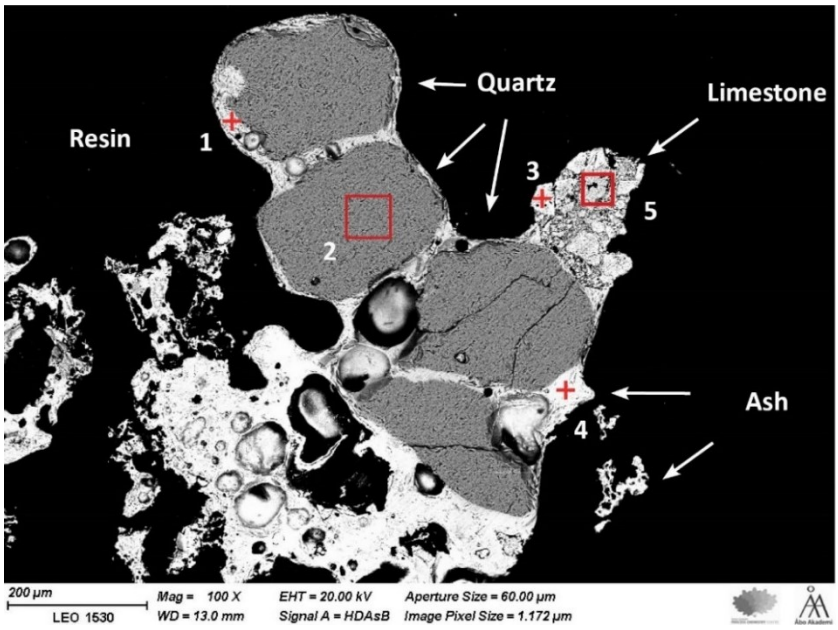

Figure 23 Image taken of bed sample collected from an experiment with 5 wt-% limestone in the bed as additive. The test ended in defluidization. A typical agglomerate contains four quartz particles bound by fuel ash. Locations marked 1–5 are EDS analyses with compositions given in Table 6 on an O-free basis.

Table 6 EDS analyses results for the points marked 1 to 5 in Figure 23.

	1	**2**	**3**	**4**	**5**
			[atomic-%]		
Na	15	-	-	1.9	-
Mg	2.0	-	1.8	24.7	0.6
Al	3.0	-	-	0.4	-
Si	58.2	100	0.2	9.1	0.3
P	2.5	-	-	13.0	-
S	-	-	1.3	1.5	-
K	37.4	-	2.5	18.6	0.2
Fe	0.5	-	-	0.8	-
Ca	7.5	-	75.0	24.0	65.8

5.4 Insights regarding sampling and analysis

The retrieval of bed material samples itself proved somewhat challenging. There were some occasions where a significant amount of bed material was lost during sampling due to the process itself. It was, however, improved throughout the work and became more reliable after some initial troubleshooting. As the preparation process preceding SEM-imaging is tedious and time-consuming, a limited number of samples were prepared. In principle, two samples were cast from every experiment: a coarse sample consisting of agglomerates and one with bed material. When exposing the cross-section of the first samples, many bubbles were revealed in the resin. This was counteracted by placing the cast samples in a vacuum to remove air bubbles. Moreover, it turned out that the samples consisting of only bed material were of little practical interest. On the other hand, second samples of agglomerates would have been helpful in cases where the casting turned out subpar. This made it challenging to obtain good images with SEM.

A more systematic approach to the qualitative comparison of EDS analyses should have been taken. Morris (2021) presents a reasonable frame of reference for such an approach. The author used a system with six different location classifications, which were then analyzed across all samples from several locations. The method provides comparability and diminishes the possibility of errors as several points are included. SEM/EDS analyses presented in this thesis are only a tiny part of the actual width of analyses made. The chosen samples were selected to be representative.

The limited operational time does, however, give a limited time for migration of the species in the bed. A limitation that Morris acknowledges as well with a similar length of experiments and even longer runs times than in this work. This meant that, for example, layering formation in the coatings could not be observed, as reported by He et al. (2016) and Visser et al. (2004).

5.5 Discussion

This experimental part of this thesis is limited to the initial phases of bed agglomeration. Depending on the viewpoint, it can also be stated that the quartz bed results in a worst-case scenario as Si is abundant and readily available to take part in the formation of melt.

Natural sand often used in commercial boilers contains less Si and should thus perform better. As there are several variables present in a full-scale boiler, there is a need for caution when applying the obtained results. Based on this work, it can only be speculated what impacts the additives have on fouling and slagging. It is, however, clear that they would have an impact downstream as well. As kaolinite bind K, Cl can form HCl instead of KCl. Work done by Aho (2001) sought to provide insight into this topic. Lab-scale tests were performed with kaolinite as an additive to study the impacts on the fouling of heat transfer surfaces. The overall conclusions were that use of kaolinite with agricultural waste is also effective against Cl-induced corrosion on superheater surfaces. This can be attributed to the fact that HCl is less harmful than KCl.

As the amount of additive is set in the experiments with it being added to the bed, the results can be viewed as a snapshot. In continuous operation, the kaolinite would have to be added continuously as it is spent. Accordingly, only indicative amounts of additives needed to prevent agglomeration can be seen in Table 3 and Table 5.

As presented in section 3.3.4, a molar ratio of 0.5 kaolinite to K should be sufficient to capture all K. The results obtained in this thesis proved that smaller ratios were enough to prevent agglomeration. No defluidization happened at a ratio of 0.4 and 0.7 kaolinite to K. The reasons for this can only be speculated, but there are some possibilities. As already mentioned, the calculations regarding the amount of K assume that all of it ends up in the bed. In reality, at least some will evaporate and end up in the fly ash. In addition, all of the K found in the fuel is not reactive. Chemical fractionation of the fuel would give a quantitative answer as water-soluble K is more prone to react.

6 Conclusions

The goal of this thesis was to find alternatives for co-firing with peat for the prevention of agglomeration. An extensive literature study was conducted, and it revealed that there are several options to prevent bed agglomeration. Successful experiments were also conducted with a lab-scale fluidized bed reactor. Two fuels, sunflower seed shells and wheat straw, along with two additives, kaolinite and limestone, were tested.

Lowering the bed temperature was found particularly effective for SFSS at tested temperatures. It is likely that wheat straw would show a similar result. The bed temperature would have had to be lowered further to achieve the threshold where melting of the ash-forming matter is limited. The commercial applicability of this is questionable as operators and boiler manufacturers want to increase efficiency with higher pressure and temperature in the steam cycle.

The effectiveness of kaolinite in preventing bed agglomeration is directly linked to the underlying agglomeration mechanism a fuel displays—the dominant agglomeration mechanisms for wheat straw are melt-induced and coating-induced for sunflower seed shells. Kaolinite prevented agglomeration more effectively in the case of coating-induced agglomeration. In the case of melt-induced agglomeration, the effect was clear but not as significant as in the coating-induced agglomeration case. At a molar ratio of 0.4 kaolinite to K, agglomeration did not occur, while a ratio of 0.3 was not enough to prevent agglomeration. In the case of wheat straw, rations of 0.9 and 1.8 only delayed agglomeration but could not prevent it.

The literature study gave a clear indication that coating-induced agglomeration would be easier to prevent than melt-induced agglomeration. This was also proven in this thesis, as discussed earlier. Further work is still needed for fuels that exhibit melt-induced agglomeration to find means to mitigate it effectively. This is particularly important as operators and manufacturers aim to increase the ratio of agricultural fuels. They often have high amounts of Si, which can be associated with a melt-induced agglomeration of fuels.

The economic feasibility of additives was not considered in this thesis, and in the end, that is the biggest driver for commercial operators. Further work would be needed in

this regard, preferably by comparing several means for the prevention of agglomeration. As there is a big drive to increase the share of “waste fuels,” such as waste-derived fuels and agricultural wastes, preventive means will be needed. It is instead a question of what works in a specific scenario.

Overall, agglomeration must be looked at in a broader context when applying the result to commercial boilers. That includes such aspects as fouling, slagging, economic feasibility, proposed fuels, and steam parameters. It is difficult to give general guidance in the form of ratios for additives as it should be studied case by case. This study gives a clear indication of the effectiveness of kaolinite that provides a starting point for more detailed engineering.

7 Summary in Swedish – Svensk sammanfattning

Förebyggande av agglomerering i samband med förbränning av biomassa i fluidiserade bäddar

Global uppvärmning har sedan länge varit ett välkänt faktum. Konsekvenserna är alarmerande och kan leda till bland annat en signifikant ökning av extrema väderfenomen, höjd havsnivå och en fallerande biodiversitet. Biomassa erbjuder en kolneutral lösning som kan ersätta utsläpp orsakade av människan härstammande från energisektorn. Kolneutraliteten motiveras genom att förbränning av biomassa bara gör en naturlig process snabbare, den skulle ske oberoende på grund av den naturliga nedbrytningen. Utnyttjande av biomassa är ändå inte helt problemfritt och förutsätter hållbara odlingsmetoder. I kombination med koldioxidlagring i anknytning till anläggningar som släpper ut koldioxid kan helheten även uppnå negativa utsläpp.

Bäddagglomerering är ett fenomen där partiklarna i en fluidiserad bädd fastnar i varandra och bildar större grupperingar, som kallas agglomerat. Det är ett allvarligt problem då man bränner biomassa med hög halt av alkalimetaller i en fluidiserad bädd. Utan förebyggande ingrepp växer agglomeraten och de ökar i mängd vilket slutligen leder till en defluidisering av bädden. Det innebär att kraftverket måste köras ner för underhåll och resulterar i märkbara kostnader. Av den orsaken har man riktat avsevärda resurser gentemot förbyggande och förståelse av fenomenet.

Biomassa och framför allt tidigare outnyttjade källor som exempelvis rester, biprodukter och avfallsbaserade bränslen är speciellt problematiska. Det beror på den relativt sett höga andelen askbildande element och askans sammansättning. Då man betraktar agglomerering blir andelen alkalimetaller och kvarts betydelsefulla: deras relativa andel är även högre i de nämnda bränsletyperna.

I litteraturen finns en stark konsensus om orsakerna till agglomerering, det orsakas av smält aska på bäddpartiklarnas yta. Den smälta beläggningen består huvudsakligen av olika silikater. Det finns två huvudsakliga mekanismer som leder till att smältan bildas. Den ena är beläggningsinducerad agglomerering, där bäddpartiklarna blir täckta av aska vilket leder till att en smält beläggning skapas. Den andra är smältinducerad

agglomerering där smältan bildas direkt på bränslepartikeln vilket leder till att bäddpartiklarna fastnar på bränslepartikeln och bildar agglomerat. I båda fallen är det kalium, natrium, kalcium och fosfor som reagerar med kvarts och bildar silikater vars smältpunkt är lägre än bäddtemperaturen i pannan.

Det finns olika metoder att förebygga agglomerering i bädden och några exempel av dessa är: additiver, kvartsfria bäddmaterial, samförbränning av olika bränslen och sänkt bäddtemperatur. Deras inverkan på specifika bränslen och de olika mekanismerna är ändå inte tydliga.

Tidigare studier har visat att samförbränning med torv effektivt förebygger agglomerering. Ca och Al-silikater har identifierats som de aktiva substanserna i torv. I detta arbete kommer additiver som innehåller de identifierande ämnena att undersökas för att bekräfta tidigare fynd och expandera kännedomen om de underliggande mekanismerna.

I detta diplomarbete utfördes en litteraturforskning för att sammanfatta den bästa tillgängliga informationen om agglomereringsmekanismerna och hur det kan undvikas. Därtill utfördes omfattande förbränningstester med en bubblande fluidiserad bädd-reaktor i laboratorieskala för att undersöka specifika bränslen och additiver. Bränslena som användes var pressade pellets gjorda av skal från solrosfrön samt pellets gjorda av halmstrå och som additiver användes kaolinit och kalksten. Bäddmaterialet i undersökningarna var kvartssand; additiverna lades till i bäddmaterialet och bäddens totala vikt var konstant i alla försök. Förbränningstesterna fortgick till defluidisering eller tills man uppnådde 500 g inmatat bränsle. Efter avslutat försök valdes agglomerat ur bädden vilka gjuts in i epoxi och de gjutna puckarna poleras för att exponera ett tvärsnitt av agglomeratet. Tvärsnitt undersöks sedan med hjälp av svepelektronmikroskop och energidispersiv röntgenspektroskopi för att bestämma sammansättningen och uppbygganden av de bildade agglomeraten och beläggningarna.

Resultaten tyder på att effektiviteten av additiverna är starkt beroende av den underliggande agglomereringsmekanismen och därmed bunden till olika bränslen. Den dominerande agglomereringsmekanismen för halmstrå var smältinducerad agglomerering och för solrosfröskal beläggningsinducerad agglomerering, vilket även var

antagandet utgående från deras sammansättning. Kaolinit förebygger agglomererering effektivt då den huvudsakliga agglomerationsmekanismen är beläggningsinducerad medan effekten är avsevärt mindre om smältinducerad agglomerering är dominerade. Bäddtemperaturens inverkan är även mer betydande då beläggningsinducerad agglomerering är dominerande. Inverkan av kalksten som additiv var låg på basen av de utförda experimenten.

Undersökningen ger goda indikationer på hur halmstrå och solrosfröskal reagerar vid förbränning i en fluidiserad bädd av kvartssand. Det praktiska implikationerna är ändå något begränsade och bör granskas i rätt kontext. Val av bränslen bör alltid betraktas ur ett helhetsperspektiv där samverkan av olika bränslen blir betydelsefull. Kraftverk opererar sällan med ett enda bränsle utan använder en blandning som bland annat varierar till följd av årstid, tillgänglighet och pris. På basis av litteraturforskningen och de utförda testen kan man ändå dra slutsatsen att kaolinit är ytterst fungerande som additiv och förebygger agglomeration effektivt.

8 References

Aho, M. (2001). Reduction of chlorine deposition in FB boilers with aluminium-containing additives. *Fuel*, *80*(13), 1943–1951. https://doi.org/10.1016/S0016-2361(01)00049-7

Barišić, V., Åmand, L.-E., & Coda Zabetta, E. (2008). The role of limestone in preventing agglomeration and slagging during CFB combustion of high phosphorus fuels. *World Bioenergy, Jönköping (Sweden)*.

Bartels, M., Nijenhuis, J., Lensselink, J., Siedlecki, M., de Jong, W., Kapteijn, F., & van Ommen, J. R. (2009). Detecting and Counteracting Agglomeration in Fluidized Bed Biomass Combustion. *Energy & Fuels*, *23*(1), 157–169. https://doi.org/10.1021/ef8005788

Basu, P. (2006). *Combustion and gasification in fluidized beds*. CRC/Taylor & Francis.

Boström, D., Skoglund, N., Grimm, A., Boman, C., Öhman, M., Broström, M., & Backman, R. (2012). Ash Transformation Chemistry during Combustion of Biomass. *Energy & Fuels*, *26*(1), 85–93. https://doi.org/10.1021/ef201205b

Brus, E., Öhman, M., & Nordin, A. (2005). Mechanisms of Bed Agglomeration during Fluidized-Bed Combustion of Biomass Fuels. *Energy & Fuels*, *19*(3), 825–832. https://doi.org/10.1021/ef0400868

Chirone, R., Miccio, F., & Scala, F. (2006). Mechanism and prediction of bed agglomeration during fluidized bed combustion of a biomass fuel: Effect of the reactor scale. *Chemical Engineering Journal*, *123*(3), 71–80. https://doi.org/10.1016/j.cej.2006.07.004

Clarke, L., Wei, Y.-M., De La Vega Navarro, A., Garg, A., Hahnmann, A. N., Khennas, S., Azevedo, I. M. L., Lösche, A., Singh, A. K., Steg, L., Strbac, G., & Wada, K. (2022). *Energy Systems. In IPCC, 2022: Climate Change 2022: Mitigation of Climate Change. Contribution of Working Group III to the Sixth Assessment Report of the Intergovernmental Panel on Climate Change [P.R. Shukla, J. Skea, R. Slade, A. Al Khourdajie, R. van Diemen, D. McCollum, M. Pathak, S. Some,*

P. Vyas, R. Fradera, M. Belkacemi, A. Hasija, G. Lisboa, S. Luz, J. Malley, (eds.)]. Cambridge University Press, Cambridge, UK and New York, NY, USA. https://www.ipcc.ch/report/ar6/wg3/

Gatternig, B., & Karl, J. (2014). The influence of particle size, fluidization velocity, and fuel type on ash-induced agglomeration in biomass combustion. *Frontiers in Energy Research*, *2*, 51.

Gatternig, B., & Karl, J. (2015). Investigations on the Mechanisms of Ash-Induced Agglomeration in Fluidized-Bed Combustion of Biomass. *Energy & Fuels*, *29*(2), 931–941. https://doi.org/10.1021/ef502658b

Geldart, D. (1972). The effect of particle size and size distribution on the behaviour of gas-fluidised beds. *Powder Technology*, *6*(4), 201–215. https://doi.org/10.1016/0032-5910(72)83014-6

Glarborg, P., & Marshall, P. (2005). Mechanism and modeling of the formation of gaseous alkali sulfates. *Combustion and Flame*, *141*(1), 22–39. https://doi.org/10.1016/j.combustflame.2004.08.014

Grimm, A., Skoglund, N., Boström, D., & Öhman, M. (2011). Bed Agglomeration Characteristics in Fluidized Quartz Bed Combustion of Phosphorus-Rich Biomass Fuels. *Energy & Fuels*, *25*(3), 937–947. https://doi.org/10.1021/ef101451e

He, H., Boström, D., & Öhman, M. (2014). Time Dependence of Bed Particle Layer Formation in Fluidized Quartz Bed Combustion of Wood-Derived Fuels. *Energy & Fuels*, *28*(6), 3841–3848. https://doi.org/10.1021/ef500386k

He, H., Ji, X., Boström, D., Backman, R., & Öhman, M. (2016). Mechanism of Quartz Bed Particle Layer Formation in Fluidized Bed Combustion of Wood-Derived Fuels. *Energy & Fuels*, *30*(3), 2227–2232. https://doi.org/10.1021/acs.energyfuels.5b02891

He, H., Skoglund, N., & Öhman, M. (2017). Time-Dependent Crack Layer Formation in Quartz Bed Particles during Fluidized Bed Combustion of Woody Biomass. *Energy & Fuels*, *31*(2), 1672–1677. https://doi.org/10.1021/acs.energyfuels.6b02980

Hupa, M. (2005). Interaction of fuels in co-firing in FBC. *Special Issue Dedicated to Professor Terry Wall*, *84*(10), 1312–1319. https://doi.org/10.1016/j.fuel.2004.07.018

Khadilkar, A. B., Rozelle, P. L., & Pisupati, S. V. (2016). Review of Particle Physics and Chemistry in Fluidized Beds for Development of Comprehensive Ash Agglomeration Prediction Models. *Energy & Fuels*, *30*(5), 3714–3734. https://doi.org/10.1021/acs.energyfuels.6b00079

Knutsson, P., Schwebel, G., Steenari, B.-M., & Leion, H. (2014). Effect of bed materials mixing on the observed bed sintering. *11th International Conference on Fluidized Bed Technology, CFB 2014; Beijing; China; 14 May 2014 through 17 May 2014*, 655–660.

Leckner, B. (2016). Fluidized Bed Combustion. In *Reference Module in Chemistry, Molecular Sciences and Chemical Engineering*. Elsevier. https://doi.org/10.1016/B978-0-12-409547-2.12183-3

Lin, W., Dam-Johansen, K., & Frandsen, F. (2003). Agglomeration in bio-fuel fired fluidized bed combustors. *Festschrift Prof. Cor M. van Den Bleek*, *96*(1), 171–185. https://doi.org/10.1016/j.cej.2003.08.008

Morris, J. D, (2021). *Mechanisms and Mitigation of Agglomeration During Fluidized Bed Combustion of Biomass*. University of Sheffield.

Morris, J. D., Daood, S. S., Chilton, S., & Nimmo, W. (2018). Mechanisms and mitigation of agglomeration during fluidized bed combustion of biomass: A review. *Fuel*, *230*, 452–473. https://doi.org/10.1016/j.fuel.2018.04.098

Nuutinen, L. H., Tiainen, M. S., Virtanen, M. E., Enestam, S. H., & Laitinen, R. S. (2004). Coating Layers on Bed Particles during Biomass Fuel Combustion in Fluidized-Bed Boilers. *Energy & Fuels*, *18*(1), 127–139. https://doi.org/10.1021/ef0300850

Öhman, M., & Nordin, A. (2000). The Role of Kaolin in Prevention of Bed Agglomeration during Fluidized Bed Combustion of Biomass Fuels. *Energy & Fuels*, *14*(3), 618–624. https://doi.org/10.1021/ef990198c

Öhman, M., Nordin, A., Skrifvars, B.-J., Backman, R., & Hupa, M. (2000). Bed agglomeration characteristics during fluidized bed combustion of biomass fuels. *Energy & Fuels*, *14*(1), 169–178.

Piotrowska, P., Grimm, A., Skoglund, N., Boman, C., Öhman, M., Zevenhoven, M., Boström, D., & Hupa, M. (2012). Fluidized-Bed Combustion of Mixtures of Rapeseed Cake and Bark: The Resulting Bed Agglomeration Characteristics. *Energy & Fuels*, *26*(4), 2028–2037. https://doi.org/10.1021/ef300130e

Raiko, R. (2002). *Poltto ja palaminen* (2. täyd. p.). Teknillistieteelliset akatemiat.

Scala, F., & Chirone, R. (2008). An SEM/EDX study of bed agglomerates formed during fluidized bed combustion of three biomass fuels. *Biomass and Bioenergy*, *32*(3), 252–266. https://doi.org/10.1016/j.biombioe.2007.09.009

Sevonius, C. (2021). Agglomeration mechanisms of a quartz bed. *Unpublished*.

Sevonius, C., Yrjas, P., & Hupa, M. (2014). Defluidization of a quartz bed–Laboratory experiments with potassium salts. *Fuel*, *127*, 161–168.

Sevonius, C., Yrjas, P., Lindberg, D., & Hupa, L. (2019). Impact of sodium salts on agglomeration in a laboratory fluidized bed. *Fuel*, *245*, 305–315.

Sevonius, C., Yrjas, P., Lindberg, D., & Hupa, L. (2020). Agglomeration tendency of a fluidized bed during addition of different phosphate compounds. *Fuel*, *268*, 117300.

Silvennoinen, J., & Hedman, M. (2013). Co-firing of agricultural fuels in a full-scale fluidized bed boiler. *Fuel Processing Technology*, *105*, 11–19.

Steenari, B.-M., Lundberg, A., Pettersson, H., Wilewska-Bien, M., & Andersson, D. (2009). Investigation of ash sintering during combustion of agricultural residues and the effect of additives. *Energy & Fuels*, *23*(11), 5655–5662.

Tropp, F. (2020). *Bed agglomeration behavior in biomass firing FBC conditions*. https://odr.chalmers.se/handle/20.500.12380/303977

Tursi, A. (2019). A review on biomass: Importance, chemistry, classification, and conversion. *Biofuel Research Journal*, *6*(2), 962–979.

Vassilev, S. V., Baxter, D., Andersen, L. K., & Vassileva, C. G. (2010). An overview of the chemical composition of biomass. *Fuel*, *89*(5), 913–933. https://doi.org/10.1016/j.fuel.2009.10.022

Vassilev, S. V., Vassileva, C. G., Song, Y.-C., Li, W.-Y., & Feng, J. (2017). Ash contents and ash-forming elements of biomass and their significance for solid biofuel combustion. *Fuel*, *208*, 377–409. https://doi.org/10.1016/j.fuel.2017.07.036

Visser, H. J. M., Kiel, J. H. A., & Veringa, H. J. (2004). *The influence of fuel composition on agglomeration behaviour in fluidised-bed combustion*. Energy research Centre of the Netherlands ECN Delft.

Wang, H., Li, C., Peng, Z., & Zhang, S. (2011). Characterization and thermal behavior of kaolin. *Journal of Thermal Analysis and Calorimetry*, *105*(1), 157–160.

Wu, S., Chen, J., Peng, D., Wu, Z., Li, Q., & Huang, T. (2019). Effects of Water Leaching on the Ash Sintering Problems of Wheat Straw. *Energies*, *12*(3). https://doi.org/10.3390/en12030387

Zevenhoven, M., Sevonius, C., Salminen, P., Lindberg, D., Brink, A., Yrjas, P., & Hupa, L. (2018). Defluidization of the oxygen carrier ilmenite–Laboratory experiments with potassium salts. *Energy*, *148*, 930–940.

Zevenhoven, M., Yrjas, P., Skrifvars, B.-J., & Hupa, M. (2012). Characterization of ash-forming matter in various solid fuels by selective leaching and its implications for fluidized-bed combustion. *Energy & Fuels*, *26*(10), 6366–6386.